1.0

2.8 2.5

3.2 2.2

3.6

4.0 2.0

1.1

1.8

1.25 1.4 1.6

MICROCOPY RESOLUTION TEST CHART
NATIONAL BUREAU OF STANDARDS 1963-A

AFWAL-TR-81-3086

A112691

LOW COST DEVELOPMENT OF INS SENSORS
FOR EXPENDABLE RPV CONTROL AND NAVIGATION

INCOSYM, Inc.
780 Lakefield Road, Suite E
Westlake Village, CA 91361

AUGUST 1981

Final Report for Period April 1979 – May 1981

DTIC FILE COPY

DTIC
ELECTE
MAR 3 1 1982

S

A

FLIGHT DYNAMICS LABORATORY
AIR FORCE WRIGHT AERONAUTICAL LABORATORIES
AIR FORCE SYSTEMS COMMAND
WRIGHT-PATTERSON AFB, OHIO 45433

82 03 30 039

NOTICE

When Government drawings, specifications, or other data are used for any purpose other than in connection with a definitely related Government procurement operation, the United States Government thereby incurs no responsibility nor any obligation whatsoever; and the fact that the government may have formulated, furnished, or in any way supplied the said drawings, specifications, or other data, is not to be regarded by implication or otherwise as in any manner licensing the holder or any other person or corporation, or conveying any rights or permission to manufacture use, or sell any patented invention that may in any way be related thereto.

This report has been reviewed by the Office of Public Affairs (ASD/PA) and is releasable to the National Technical Information Service (NTIS). At NTIS, it will be available to the general public, including foreign nations.

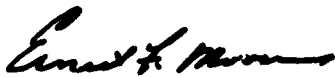This technical report has been reviewed and is approved for publication.

J. VAN ROBERTS
Project Engineer
Control Data Group
Control Systems Development Branch

EVARD H. FLINN, Chief
Control Systems Development Branch
Flight Control Division

FOR THE COMMANDER

ERNEST F. MOORE, COLONEL, USAF
Chief, Flight Control Division

REPORT DOCUMENTATION PAGE		READ INSTRUCTIONS BEFORE COMPLETING FORM
1. REPORT NUMBER AFWAL-TR-81-3086	2. GOVT ACCESSION NO. AD-A11269 1	3. RECIPIENT'S CATALOG NUMBER
4. TITLE *(and Subtitle)* LOW COST DEVELOPMENT OF INS SENSORS FOR EXPENDABLE RPV CONTROL AND NAVIGATION		5. TYPE OF REPORT & PERIOD COVERED Final – April 1979 to May 1981
		6. PERFORMING ORG. REPORT NUMBER
7. AUTHOR(s) D.G. Kim James G. Russell		8. CONTRACT OR GRANT NUMBER(s) F-33615-79-C-3616
9. PERFORMING ORGANIZATION NAME AND ADDRESS INCOSYM, Inc. 780 Lakefield Road - Suite E Westlake Village, CA 91361		10. PROGRAM ELEMENT, PROJECT, TASK AREA & WORK UNIT NUMBERS 56-100/200
11. CONTROLLING OFFICE NAME AND ADDRESS Flight Dynamics Laboratory (AFWAL/FIGL) Air Force Wright Aeronautical Laboratories (AFSC) Wright-Patterson Air Force Base		12. REPORT DATE August 1981
		13. NUMBER OF PAGES 62
14. MONITORING AGENCY NAME & ADDRESS*(if different from Controlling Office)*		15. SECURITY CLASS. *(of this report)* UNCLASSIFIED
		15a. DECLASSIFICATION/DOWNGRADING SCHEDULE

16. DISTRIBUTION STATEMENT *(of this Report)*

Approved for public release; distribution unlimited.

17. DISTRIBUTION STATEMENT *(of the abstract entered in Block 20, if different from Report)*

18. SUPPLEMENTARY NOTES

19. KEY WORDS *(Continue on reverse side if necessary and identify by block number)*

Magnetic Field	Navi?	Scale Factor	Remotely Piloted
Rotating	Frequ? ?k	Bias	Vehicle
Slip Rings	Coil	Heading	
Acceleration	Non-Linearity	Unstable	

20. ABSTRACT *(Continue on reverse side if necessary and identify by block number)*

A two year development effort has resulted in the design, fabrication and test of a feasibility model 3-axis vibrating beam accelerometer and a brassboard cycloidal magnetic vector sensor. The cycloidal magnetic vector sensor is based on a rotating coil technique which eliminates slip rings. It performed as expected, and demonstrated an accuracy of approximately 0.25 degrees.

DD FORM 1473 EDITION OF 1 NOV 68 IS OBSOLETE
1 JAN 73

20. Abstract (continued)

The 3-axis vibrating beam accelerometer is based on the principle that a vibrating beam will change its frequency as a function of the applied tension. Using six beams, two per sensing axis, connected to a common mass, a 3-axis accelerometer can be designed. Such a design measures acceleration, by a change in beam vibration frequency, as a function of applied acceleration to the mass.

The accelerometer, at first, demonstrated an insensitivity due to frequency lock between the beams. This effect was eliminated, but the necessary change in design caused an unstable bias and non-linearity of the scale factor. A solution to these problems was also conceived, and hardware changes made. However, to fully demonstrate the concept requires a computer and software, which is outside the scope of this program.

PREFACE

TABLE OF CONTENTS

TABLE OF CONTENTS (continued)

LIST OF ILLUSTRATIONS

LIST OF TABLES

SUMMARY

A two-year development effort has resulted in a designed, fabricated, and tested feasibility model of a 3-axis vibrating beam accelerometer. Also the work started by the Flight Dynamics Laboratory on a Cycloidal Magnetic Vector Sensor (CMVS) was continued and a brassboard model was designed, fabricated and tested. Electronics for both were designed and breadboarded, and utilized in the testing of the instruments. The CMVS is based on a rotating coil technique but without slip rings. Two coils are rotated with their sensing axes at 90 degrees to each other. A connecting wire is used in place of a slip ring, and is connected in such a manner as to not "wind up".

The CMVS data showed that the performance was better than magnetic heading devices presently available. The magnetic heading error shown by test was approximately 1/4 of a degree, which would be adequate for RPV navigation of $\pm 5\%$ accuracy over a 200 mile range, which was the goal performance for the CMVS.

The 3-axis vibrating beam accelerometer was developed to the point of demonstrating the feasibility of acceleration measurement with a simple design. The concept used was to connect six beams to a common mass. Two beams support the mass along each of its axes. These beams are vibrated by electromagnetic drivers. When an acceleration is applied to the mass, the beams will change their oscillation frequency as a function of the acceleration. The beam oscillation frequency is sensed, and the change in frequency between the two beams on any axis is used as a measure of acceleration.

The fundamental limitation to this device is the tendency of the beams to lock when operated at a common frequency (frequency lock) due to energy transmission from one to the other through the common mass, and/or the case. This causes no output to occur for low levels of acceleration. To avoid this limitation the beam dimensions and tensions were varied so that they operated at different frequencies. This method resolved the frequency lock, but caused the scale factor to be non-linear and the bias unstable. A method was devised to remedy both of these deficiencies. However, the modification requires computation capability be connected to the accelerometer electronics, and a suitable computer or software was not planned or available under this program.

Further work will be required to implement the above changes, and until then the accelerometer is not accurate enough for navigation requirements.

SECTION I

INTRODUCTION AND BACKGROUND

1.1   BACKGROUND

In April 1979, INCOSYM was awarded Air Force Contract F33615-79-C-3616 to demonstrate the feasibility of a vibratory 3-axis accelerometer and continue the development of a Cycloidal Magnetic Vector Sensor (CMVS). The reason for performing this development is the possibility of providing heading, acceleration and rate measurement capability as a low cost for control and navigation of expendable Remotely Piloted Vehicles (RPVs).

Current techniques for RPV flight control do not include autonomous navigation, and current autonomous navigation systems are too expensive for expendable RPVs. Recent research and development within the Air Force in the area of low cost sensors has resulted in demonstrations of several instrument techniques, including a cycloidal magnetic vector sensor. In 1976-77, a crude cycloidal motion magnetic sensor was invented and demonstrated by the Flight Dynamics Lab. Sensing elements are rotated without the use of slip rings, in an inherently low cost design, to obtain a magnetic vector. It appeared that with some sensor design refinement, the resulting magnetic vector could be used as a combined control and heading sensor for RPVs. Since only basic operation of the cycloidal magnetic sensor was demonstrated by the Flight Dynamics Lab, a brassboard effort was performed during this program to determine its capacity to meet RPV system requirements. Also, it is recognized that an accelerometer of sufficient low cost and performance is required to complement the cycloidal motion sensor and form an autonomous navigation system. Specifically, a unique and proprietary 3-axis vibrating beam accelerometer is recognized as having significant potential in meeting the cost and performance objectives of this effort. The effort under this program investigated the feasibility of a unique 3-axis accelerometer principle which could be simpler and less expensive than conventional inertial sensors due to a unique single inertial mass, beam suspension, electronic oscillation techniques, and an inherently digital output.

1

1.2   INTRODUCTION

The 3-axis vibrating beam accelerometer is based on a concept which utilizes six (6) beams connected to a common proof mass. Each axis consists of two (2) beams that are colinear, with one end of each beam connected to the proof mass and the other end to a common housing. Each of the resultant three axes are orthogonal to the other two. Two methods of driving and sensing the beam oscillation were considered. One was to drive and sense the oscillations by means of piezoelectric substrates bonded to the beams. The other method was to drive and sense the oscillations by utilizing the electro-magnetic properties generated when a current is applied through a coil. The latter approach was found to be the better because the damping of the oscillation caused by the piezoelectrics when bonded to the beams reduces the sensitivity of the device.

The first feasibility model designed was considered too complex to fabricate for low cost during the preliminary design review. Consequently, the design was simplified considerably, without compromising the basic operation. This design was then fabricated and tested. Initially, "frequency lock" between the beams (a condition described in Section 2.0) caused a threshold level which was higher than desirable. To eliminate the threshold, the beams were operated at different frequencies. This was accomplished by utilizing two different beam thicknesses, and then adding an electronic bias to set the exact frequency of oscillation. Using different beam thicknesses, however, caused a nonlinearity of the scale factor and bias changes during operation. Subsequently, a method of applying the electronic bias was devised which would reduce bias changes and linearize the scale factor, while at the same time setting each beam oscillation at a unique frequency. The bias drive electronics to perform this technique were included in the design. However, to correct for non-linearity effects and bias changes, the electronics require some computation which would normally be performed by the navigation computer. As this program only addressed the sensor development, the required computation capability was not available.

One other factor was resolved by operating the beams with an electronic bias. When a beam is driven with a sinusoidal magnetic flux, it will naturally oscillate at twice the frequency of the current input. By application of a DC electronic bias, the beam can be made to operate at the same

frequency as the driving current. It is possible to select the unique frequency for the beams and to obtain operation at the fundamental frequency without computation capability so these adjustments were included in the feasibility model.

The basic operation of the feasibility model was as predicted after some experience was gained in setting the mechanical tension of the beams and some improvements were made to the electronics design.

Due to the fact that the computational capability to reduce the bias shifts was not available, the test data obtained were not accurate enough for navigation purposes.

The cycloidal magnetic vector sensor was based on the same principle as that shown in the feasibility model built by the Flight Dynamics Lab. Early testing, however, showed a short life span (20 or 30 hours) for the wires that connect to the rotating coils. After various types of wire had been tried without significant improvement, a coil type connection was developed. It became apparent after considerable trial and error that the coil dimensioning and the configuration of the grooving as it passes through the gear drive are important for long life operation. To alleviate the effects of the DC drive motor on the operation of the CMVS, it was mounted at approximately five inches from the coils. This made the CMVS larger (it is approximately seven inches long) than originally envisioned but the motor does not affect the performance. One factor which did cause a slight effect on the performance was the use of standard ball bearings as the rotational support for the coils. These bearings have magnetic properties that cause a very small deviation of the input magnetic field. The error is only 0.1 to 0.2 degrees of the magnetic heading vector. However, it appears to be the major error contributor, as the errors of the CMVS were only about 0.3 degrees. This effect could be eliminated by using a non-magnetic bearing.

The performance of the CMVS was good and it could be used, with some repackaging to make it flight worthy, for a RPV heading reference. It appears to be more accurate than presently available magnetic heading instruments.

SECTION II

THEORY OF OPERATION OF THE THREE AXIS VIBRATING BEAM ACCELEROMETER

If a mass is supported by a vibrating suspension, any force on the mass will change the vibration frequency of the suspension. If the mass is exposed to acceleration then a force is induced on the mass, and the change in vibration frequency of the suspension is a measure of acceleration. By utilizing this effect, an accelerometer can be designed.

The mechanization used for the design for this program is as follows. A mass is supported by six beams as shown in Figure 1. If the beams are vibrated, any acceleration input to the mass will change the frequencies of vibration of the beams. For the component of acceleration along any axis, one beam will be put in tension and its vibration frequency will increase, and the other beam will be put in compression and its vibration frequency will decrease. Therefore, the output on each axis is the algebraic difference between the change in vibrating frequencies of the two beams. The two beams on any axis can be tuned to the same frequency, in which case subtracting one signal from the other with no acceleration will give a zero output, i.e., there would be no bias term. However, the problem with operating the beams at the same frequency is their tendency to "frequency lock". This is due to the energy being dissipated by the vibration being in phase and at the same frequency for each beam. This results in both beams staying at the same frequency even under acceleration inputs, and so no output occurs. This effect results in a threshold level. One way to resolve this is to run the beams at different frequencies, and this approach was taken. This results in a fixed bias output, but this is stored in the system computer as is presently done on systems. Operation at different frequencies also resulted in a non-linear output, but a method of resolving this problem is described in Section 3.2.

Various materials were considered for the beams. One approach was to bond two piezoelectric beams together. A voltage is applied to one side to drive the beam, and the output generated from the bending motion of the other piezoelectric beam is used to sense the amplitude of vibration. However the inherent damping caused by such a beam structure is too high to give

4
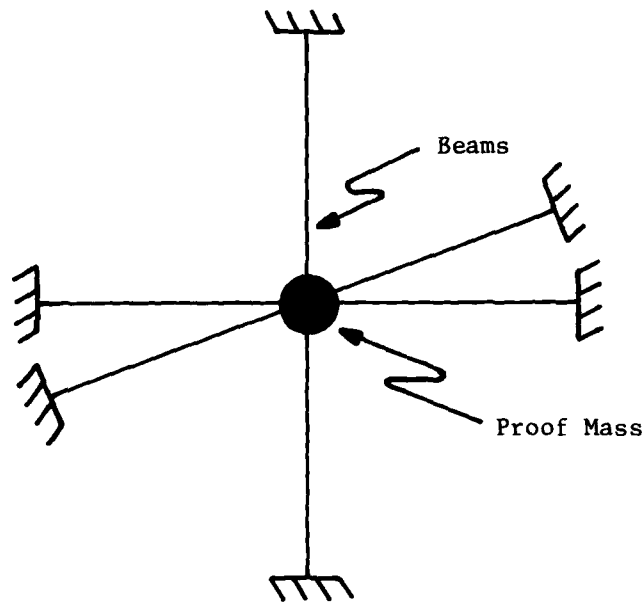
All beams are at 90° to each other.

Figure 1. Schematic of the Three Axis Vibrating Beam
Accelerometer

good sensitivity. Instead, metal beams were used and driven electromag-
netically by current through a coil. A second coil is generally used to
sense the amplitude of vibration. However, in the design developed under
this contract it was found that one coil could be used for both driving and
sensing the vibration of the beam. *Using one coil also allowed better opera-
tion as it eliminated the magnetic feedback between the coils.* The output
from the sensing coils are amplified, and the input acceleration is computed
as f_1 minus f_2, where f_1 and f_2 are the outputs from any pair of beams. When
the beams are not at the same resonance, so that the "lock-in" is avoided,
then even with zero input there will be an output. This is the fixed bias.

5

The advantages of such a mechanization are:

(a) Three (3) axes from one instrument.

(b) Very few parts and simple electronics.

(c) The output is digital, so no conversion is necessary.

(d) As the beams are similar and have the same characteristics, and as the output is the difference in frequency between beams, long term and thermal bias effects tend to cancel.

(e) Rugged because for any shock or acceleration input, at least one beam is in tension to support the mass. In tension, the beams are very strong.
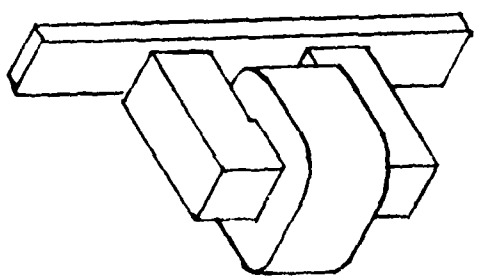
Driver Assembly
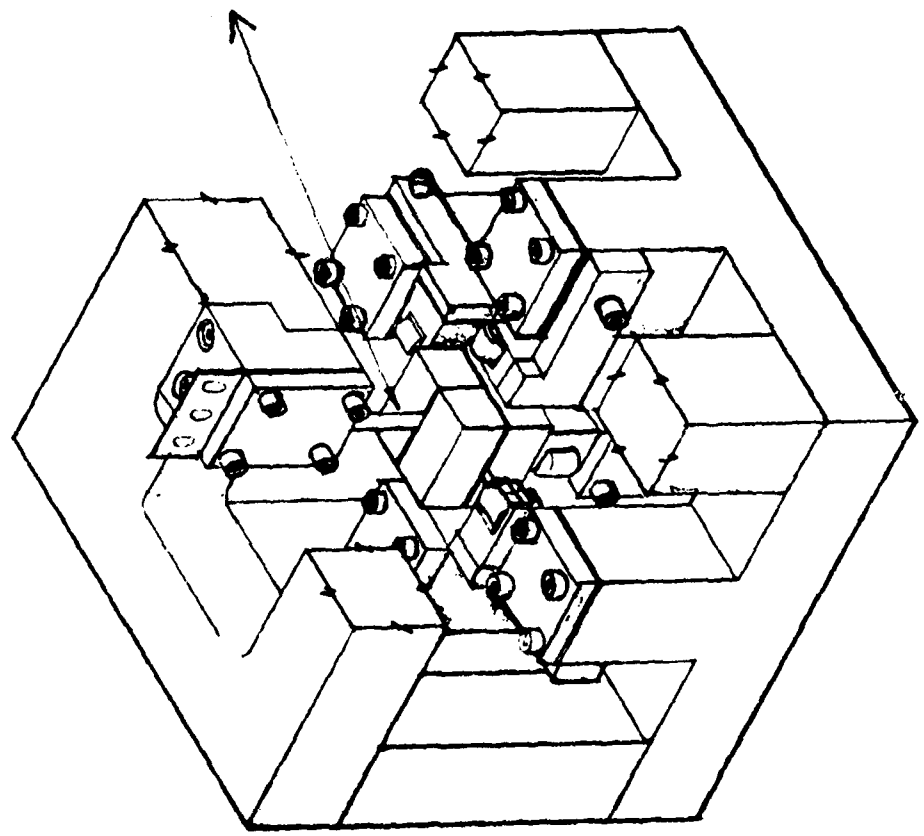
Figure 2. Cutout View of the 3-Axis Accelerometer

7

SECTION III

DESIGN OF THE THREE AXIS VIBRATING BEAM ACCELEROMETER

3.1   GENERAL DESCRIPTION

Six separate beams are each vibrated by applying a sinusoidal electromagnetic field at their resonant frequencies. The six beams are orientated so that each set of two are aligned with their longitudinal axis colinear on each of the three cardinal axes of the instrument. A proof mass is supported by the six beams as shown in Figure 2. The beams are fastened at each end to an outer case. The electromagnetic field is generated by applying a sinusoidal current through a coil. The coil is wound on a laminated C core so that the generated field can be controlled and directed in a way to drive the beams. The vibrating motion of the beams is sensed by the same coil. The output of the coil is amplified and the difference in frequency between any two colinear beams is measured. The C core is fastened to the case of the accelerometer.

3.2   BEAM CONSTRUCTION

The beams were made on an Electrical Discharge Machine (EDM) from 0.005 inch thick 1095 steel sheet. The tension can be adjusted for each beam, and then the holding screws tightened. This eliminates the need for close dimensional control of the beam dimensions. It also allows the beams to be set at different frequencies so that the "frequency-lock" problem can be eliminated. "Frequency-lock" is a problem in any vibrating beam type of mechanism and especially when there are three axes (6 beams) involved. The six separate elements should vibrate independently within a specified input acceleration range.

The beam resonance frequency may be calculated from the static deflection:

$$f_n = 3.622 \left(\frac{1}{Y_{max}}\right)^{1/2} \qquad (3-1)$$

where Y_{max} (the deflection) for a uniformly loaded beam clamped at both ends can be expressed as:

$$Y_{max} = -\frac{Wj^2}{\delta T} \left[\frac{4U \left(1-\cos h \frac{1}{2} U\right)}{\sin h \frac{1}{2} U} + U^2 \right] \qquad (3-2)$$

where

$$j = \sqrt{\frac{EI}{T}}$$

$$U = \frac{L}{j}$$

$$I = \frac{bt^2}{12}$$

$$W = \rho \, bt$$

and

E = Modulus of elasticity, lb/in^2

I = Moment of inertia, in^4

P = Tension, lb

l = Length of the beam, in

b = Width of the beam, in

t = Thickness of the beam, in

ρ = Mass per unit area, $lb \ sec^2/in^3$

Ideally, six frequencies can be calculated such that minimum inter-ference between beams can be achieved. However, in practice it is difficult to maintain these calculated frequencies for all six beams. The vibrating frequencies can be separated by constructing beams of all different sizes, such that for a given tension individual beams are operated at separated

9

frequencies. This technique requires manufacturing precise dimensions for beams of six different sizes. It is advantageous to limit sizes of the beams to a minimum number for manufacturing purposes. As the individual axes have provisions to control the tension, two beam sizes were chosen such that separation of the frequencies is sufficient to avoid any "frequency-lock". Beams of approximately 0.04 and 0.05 inches wide were chosen for each of the beams in any axis, and then the tension adjusted in test. Figure 3 shows the relationship between frequency and tension for each of these sizes. A separation in resonant frequency of approximately 0.5 kHz occurs for these beam sizes if the tension is set at 3 pounds on each. The desired bandwidth of each frequency is approximately ±160 Hz to cover ±20 g input range. The difference (range) between the highest and lowest frequency for the beams is approximately 600 Hz. This frequency spread is equivalent to about 10% of the nominal frequency of 6 kHz. This number is important in designing a tuning circuit whose component tolerance is $\pm10\%$, as this reduces the amount of special tuning required for each beam. A fine adjustment, so that each beam is at an integral frequency, can be accomplished in the electronics, as described in Section VI.

Examination of Figure 3 indicates that the change in frequency as a function of tension is not the same for the two beam widths. This means that as the tension changes due to acceleration on the proof mass or any other cause, then $f_1 - f_2$ is not linear.

To demonstrate the operation of the beams it is easier to analyze the effect of a change in tension on a string. String equations are easier to use because the string vibration is virtually unaffected by the end damping conditions, whereas the beam is strongly affected. However, the cause and affect from a change in tension is the same.

The resultant frequencies of two strings as a function of longitudinally applied tension may be expressed as:

$$f_1{}^2 = \frac{T_1}{4\sigma_1, \ E^2} \qquad (3\text{-}3)$$

$$f_2{}^2 = \frac{T_2}{4\sigma_2, \ E^2} \qquad (3\text{-}4)$$

10
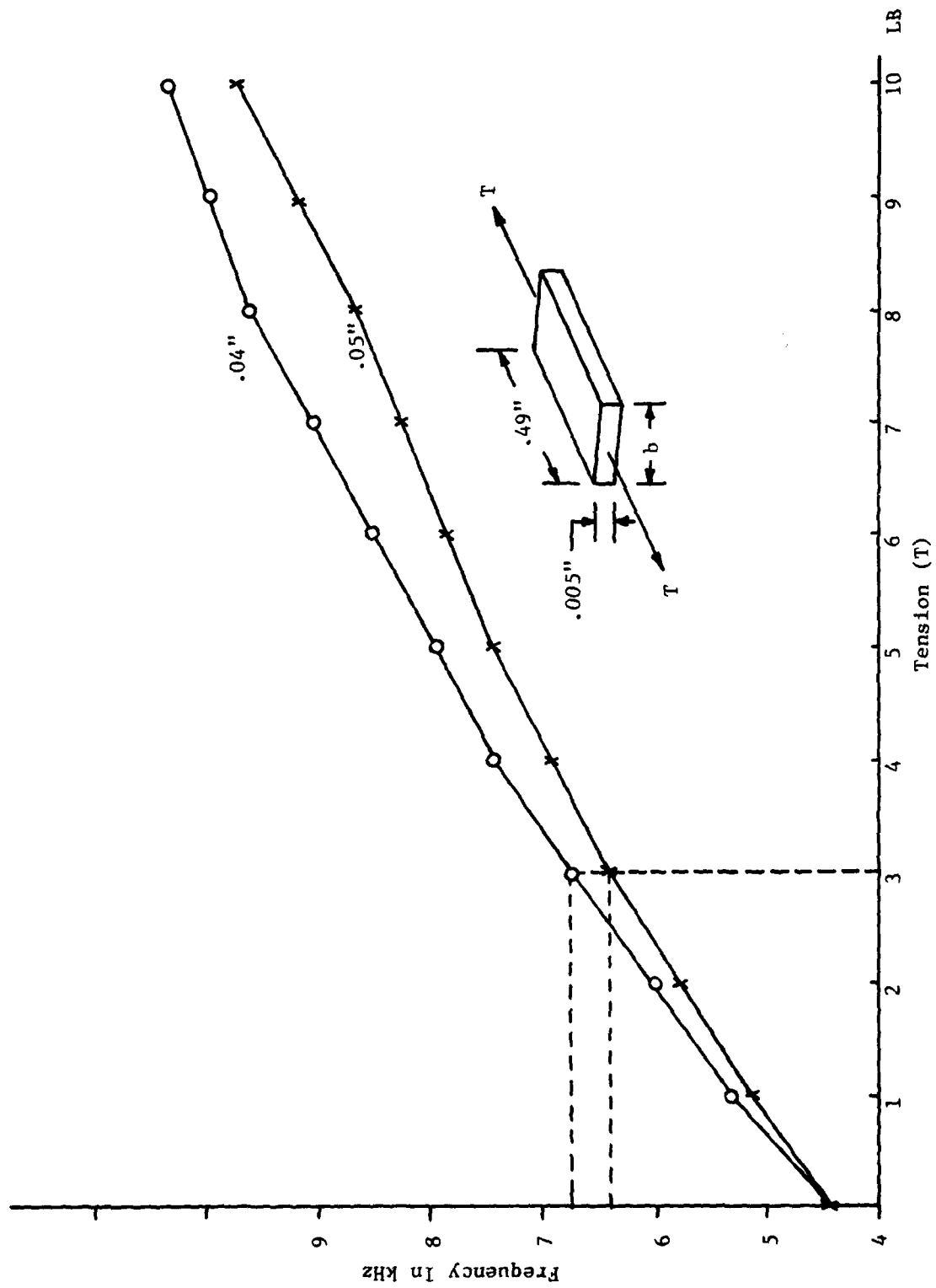
Figure 3. Vibrating Frequency Versus Tension for Two Beam Widths

where :

f_1 and f_2 are the frequencies of strings 1 and 2

σ_1 and σ_2 is the mass for unit length of strings 1 and 2

E is the length of the strings (both the same)

T_1 and T_2 is the tension applied to strings 1 and 2

.... acceleration along the axis of the strings, a change in tens.... .. ... which is equal to the proof mass times acceleration (M A). Therefore

$$T_1 - T_2 = M A \qquad (3\text{-}5)$$

If σ_1 had been made equal to σ_2, then the difference frequency from equation 3-3 and 3-4 would be

$$f_1{}^2 - f_2{}^2 = \frac{T_1 - T_2}{4\sigma, E^2} \qquad (3\text{-}6)$$

Substituting Equation 3-5, Equation 3-6 can be written

$$f_1 - f_2 = \frac{M A}{(f_1 + f_2)\ 4\sigma\ E^2} \qquad (3\text{-}7)$$

However, because of the difference between σ_1 and σ_2 (caused by design to cure the "frequency-lock"), Equation 3-7 does not correctly describe the output, and in fact a non-linear output results.

Examination of Figure 3 shows that in fact two sources of error occur because of the difference in beam widths. First, as the tension increases as a function of the acceleration input, the two beams do not

12

"track", resulting in the difference frequency, f_1-f_2, being non-linear. This results in the scale factor of the accelerometer being non-linear. Also, if the tension changes without any acceleration input, e.g., changes caused by thermal effects etc., then the output (f_1-f_2) of the instrument changes with no input, which is a change in the bias.

Consequently, a method was devised to resolve this deficiency. As the mechanization of the accelerometer and its electronics measures the frequency from each beam as the required outputs, then these two frequencies can be used to measure the tension in each beam.

$$T_1 = f_1^2 \ 4\sigma_1 \ E^2$$

$$T_2 = f_2^2 \ 4\sigma_2 \ E^2$$

The sum of the two tensions are:

$$T_1 + T_2 = 4 \ E^2 \ (\sigma_1 f_1^2 + \sigma_2 f_2^2) \tag{3-8}$$

The method described in Section VI that applies a force to the beam by passing DC current through the coil for fine frequency adjustment can also be utilized at the same time and is the same way to apply a force that is a function of T_1 and T_2. If $T_1 + T_2$ is computed, as per Equation 3-8, and a force applied to each beam to keep $T_1 + T_2$ constant, then the scale factor is a linear function of input acceleration, and the bias will stay constant. However, as implementation of this technique requires a computer, which would be part of the system used in the vehicle, it was not tested under this program.

3.3 COIL

Initially, the driver and pickoff coils were separate coils wound on the same lamination. However, it was discovered when testing the breadboard that having two separate coils did not operate the device successfully. This was due to magnetic field feedback between the driver and sensing coil,

and the difficulty of maintaining the necessary phase margin for demodulation
of the sensing signal. Various methods of alleviating these problems were
tried, but eventually the coil design and electronics were modified, and a
single coil was used to both drive the beam and sense the resultant motion.
This mechanization resulted in simplifying both the coil and electronics.
The resultant coil consisted of 400 turns of size 46 AWG wire wound on a
laminated C core. The laminates are 0.002 inch thick Hy-Mu 80. The wire
insulation is Polyvinyl Formel (Formvar).

3.4   HOUSING

The housing is made of one piece. It consists of the base plate,
which is the mounting surface of the accelerometer, and four posts all made
as one piece. The four posts have the required hole patterns so that the
beams and coils can be attached to them. A top plate and four more posts are
made as separate pieces and fastened to the housing, along with the beams,
proof mass and coils, to complete the assembly. The housing, the plate and
posts are all machined from C 1018 steel.

SECTION IV

THEORY OF OPERATION OF THE CYCLOIDAL MAGNETIC VECTOR SENSOR

4.1 GENERAL OPERATION

In 1976-77, a breadboard magnetic sensor referred to as a "Cycloidal Magnetic Vector Sensor (CMVS)" was demonstrated by FGL/Flight Dynamics Laboratory AFWAL, Wright-Patterson AFB, Ohio. The CMVS is a rotating magnetic field sensor of the type of device often referred to as a magnetometer. A magnetometer is a device that utilizes Faraday's Law of Electromagnetic Induction to measure a magnetic field. This law states that a current can be induced in a coil by a change in a magnetic field. A magnetometer is generally used to measure the earth's magnetic field. There are two general approaches, and the major difference is that in one method the coils rotate and in the other the coils are stationary. The stationary mechanization is often referred to as a "flux gate". The main reason a rotating approach has not been used in the past is that a method had not been devised to eliminate slip rings. The slip rings produced too much electrical noise and reduced life. However, the work done at the Flight Dynamics Lab indicates that slip rings could be eliminated. By adaptation of this technique two coils can be rotated, providing three (3) axes of information. The major advantages of the technique described in the following pages are:

    (a) No slip rings, which eliminates electrical noise and improves life.

    (b) Three dimensional information from a simple planar rotation.

    (c) No external reference signal required as is necessary for a stationary coil design as the reference signal is self-generated in the coils.

    (d) Very simple mechanical construction and few electrical components, resulting in potentially low cost and long life.

4.2 CHARACTERISTICS OF THE CMVS

Faraday's Law of Electromagnetic Induction states that the induced voltage in a closed loop conductor is proportional to the rate-of-change of the magnetic flux linkage to the loop.

Expressed mathematically:

$$E = \frac{d\phi}{dt} = \frac{d}{dt} (\vec{B} \cdot \vec{S})$$

where:

E = the voltage induced in the loop

ϕ = the magnetic flux passing through the loop

$\vec{B}$ = is the flux density vector

$\vec{S}$ = is the loop area vector

A rotating single loop between a pair of magnetic poles generates an electrical voltage whose amplitude is $E = B \cdot S \sin wt$. Such a configuration is a basic generator. When the loop is perpendicular to the magnetic flux lines, the induced voltage is zero. When the loop is parallel to the direction of the magnetic flux lines, the induced voltage is a maximum.

A loop which is rotated in the geomagnetic field will behave in the same way. If the loop area vector $\vec{S}$ is approximately perpendicular to the earth's gravity vector, a maximum voltage will occur as $\vec{S}$ points East and West and zero as it points in the direction of the magnetic poles.

The earth's magnetic field has both vertical and horizontal components. The direction of the horizontal component is magnetic north and south, and the vertical component indicates the direction of gravity. These two pieces of information can be utilized to determine heading and attitude of a vehicle.

In the past, the accuracy and life of a rotating magnetometer has been limited because of the requirement of utilizing slip rings to transport the electrical signals between the rotating and nonrotat ng parts of the device. Slip rings generated too much electrical noise relative to the signal. However, a method of eliminating the slip rings is available by designing the magnetometer in the following manner.

As a wire (or flexible cable) will not "wind up" when both ends turn in the same direction by an equal amount, the CMVS coils are rotated at one end of the cable once for each rotation of the drive mechanism. In this

way, the cable will never get twisted. The drive end of the cable can be terminated in a gear which can be driven by a DC motor or other drive source.

When a DC motor is used, the magnetic field generated by the motor must be eliminated from the magnetometer signal. This must be accomplished in such a way as to not distort the earth's magnetic field relative to the measurement coils. Therefore, when shielding is used it must be applied in a manner that will not cause significant distortion of the earth's magnetic field, or if it does, distortion occurs in a predictable way that is eliminated by the signal processing of the device. Because the coils are rotating, it is possible to determine the distortion of the earth's field by examination of the output of the coils when they are 180° apart.

The signal strength from this kind of magnetometer can be relatively large. For example, if a coil (loop) is utilized that has a thousand (1,000) turns and has an area of 16×10^{-4} meters^2, and rotates at 100 Hz, the output voltage will be 50 millivolts per gauss.

4.3   SIGNAL WAVEFORMS OF THE CMVS

A sensing loop in a Cartesian coordinate X Y Z illustrated in Figure 4 has an area vector S with its original direction parallel to the axis. The area vector S, when rotated at a velocity of wt, can be expressed as:

$$S_x = - S \cos wt \sin wt$$

$$S_y = S \cos wt \cos wt$$
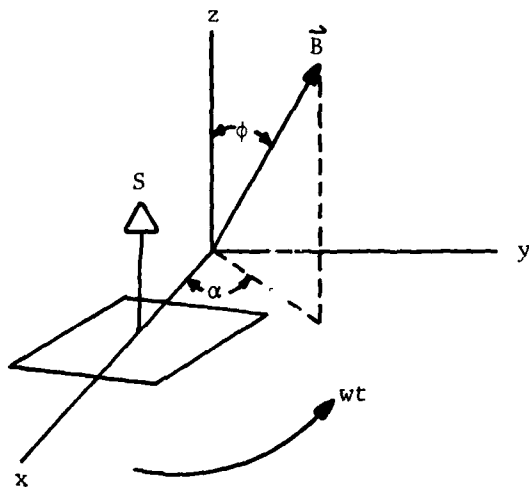
$$S_z = S \cos wt$$

If we assume a steady homogeneous magnetic field the components are:

$$B_x = B \sin \phi \cos \alpha$$

$$B_y = B \sin \phi \sin \alpha$$

$$B_z = B \cos \phi$$

Figure 4

17

where ϕ is the angle between the Z axis and the $\vec{B}$ vector, α is the angle between the X axis and the X-Y plane projection of the $\vec{B}$ vector.

The output EMF is

$$E = -\frac{d}{dt} (\vec{S} \cdot \vec{B})$$

$$= -Sw (-B_x \cos 2wt - B_y \sin 2wt - B_z \sin wt)$$

$$= -SwB (-\sin \phi \cos (\alpha - 2wt) - \cos \phi \sin wt) \qquad (4-1)$$

The second loop may be added to the system with an area vector originally pointing along the X axis (see Figure 5). The output will be

$$E = -SwB \sin \phi \sin (\alpha - wt) \qquad (4-2)$$

Figure 5

From equations (4-1) and (4-2), we can generate the following vectors:

(a) $E_1 = -\sin \phi \cos (2 wt - \alpha)$ (4-3)

(b) $E_2 = -\sin \phi \sin (\alpha - wt)$ (4-4)

(c) $E_3 = -\cos \phi \sin (wt)$ (4-5)

These vectors are the components of the magnetic field.
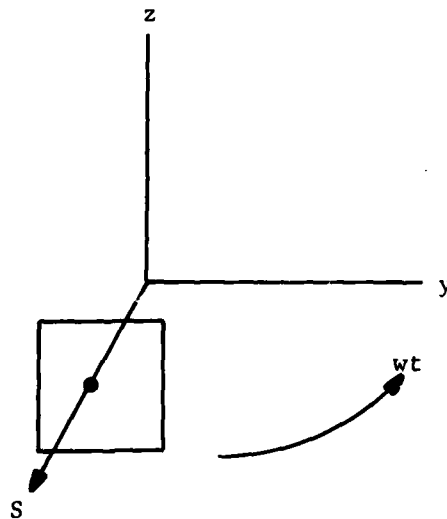
SECTION V

DESIGN OF THE CYCLOIDAL MAGNETIC VECTOR SENSOR (CMVS)

5.1 GENERAL DESCRIPTION

The Cycloidal Magnetic Vector Sensor (CMVS) consists of two sets of coils, each set being mounted on a bevel gear. Both bevel gears are rotated by a common shaft which is driven from a DC motor. In this manner, both sets of coils are rotated by the DC motor. Each set of coils consists of two separate windings which are assembled so that their measurement planes are at 90 degrees to each other. Both sets of gears/coils are mounted diametrically opposite to each other. The mechanization is shown in Figure 6. The device could have been fabricated with only one set of coils, consisting of two windings with their measurement axis 90 degrees apart, but two sets were used so that two windings (one on each side of the shaft) could be wired together in series to provide twice the sensitivity, and at the same time provide a balanced mass on the shaft.

To connect the rotating windings of each set of coils to the outside world (case) slip rings could be used. However, because of the low signal level generated by the coils and the inherent failure rate of slip rings, a more optimum approach is to provide direct electrical connection through wires. In mechanizing this direct coupling, the objective is to prevent the wires from "winding up". This is accomplished by routing the connecting wires through the center of the bevel gears and through a 90 degree angle between the case and the coils. Now as the coils rotate on the bevel gears they start to "wind up" the connecting wires but because the bevel gear mechanism is rotating with the shaft, and as both shaft and coil rotate at the same speed i.e., one rotation of the gear/shaft combination unwinds (turn-for-turn) the "wind up" caused by the coil rotation.

The rotating windings described, which have their measurement axes 90 degrees apart, are diagrammed in Figure 7. One set of windings is referred to as the vertical sensing, and the other the horizontal sensing.

The challenge in this approach is to design the mechanism so that the wind/unwind motion does not cause fatigue failures in the connecting wires. The CMVS design built for this contract and described in the following section was successful in accomplishing this objective.

20
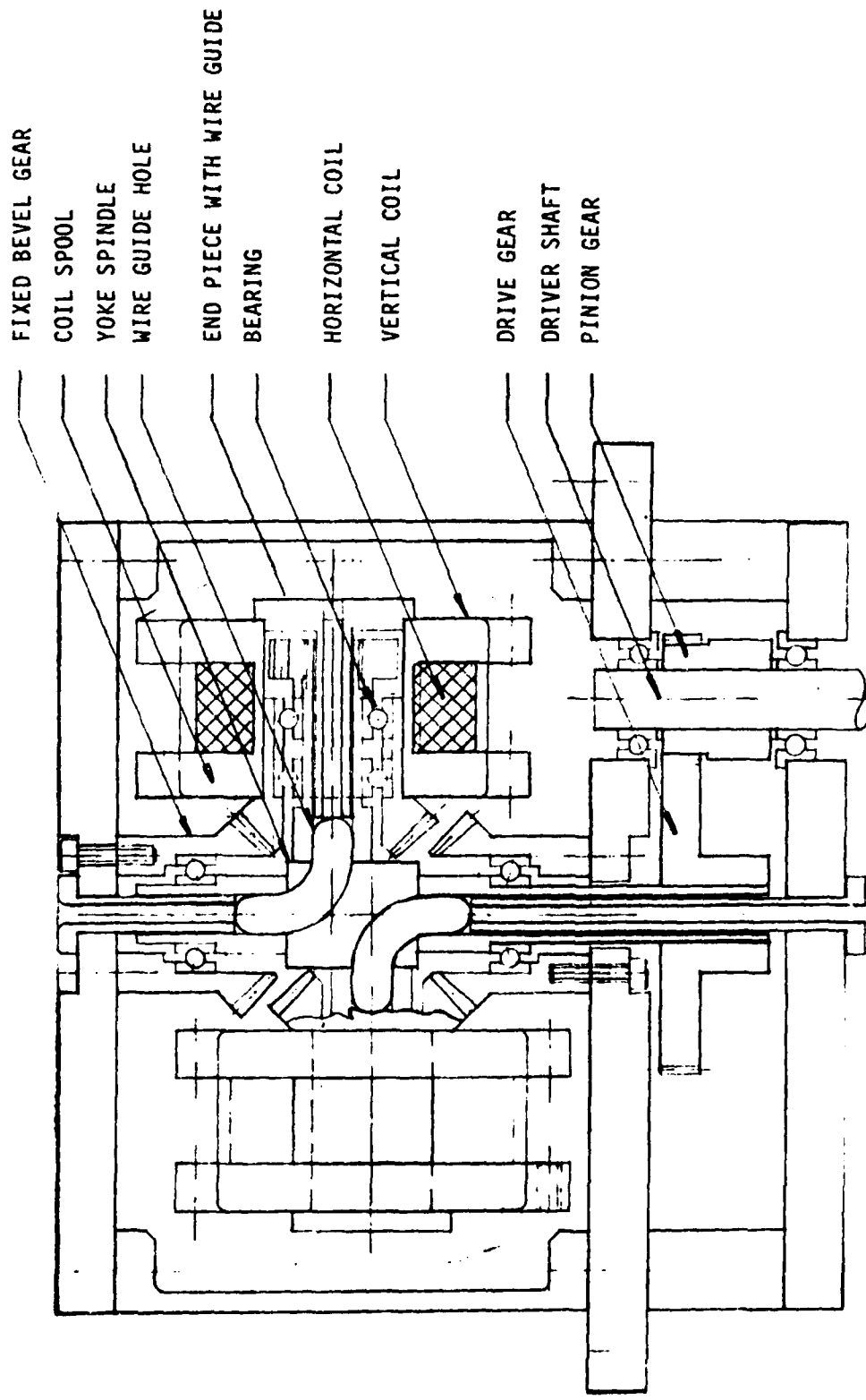
FIXED BEVEL GEAR

COIL SPOOL

YOKE SPINDLE

WIRE GUIDE HOLE

END PIECE WITH WIRE GUIDE

BEARING

HORIZONTAL COIL

VERTICAL COIL

DRIVE GEAR

DRIVER SHAFT

PINION GEAR

Figure 6. Cutout View of Cycloidal Magnetic Vector Sensor

21

HORIZONTAL SENSOR

VERTICAL SENSOR
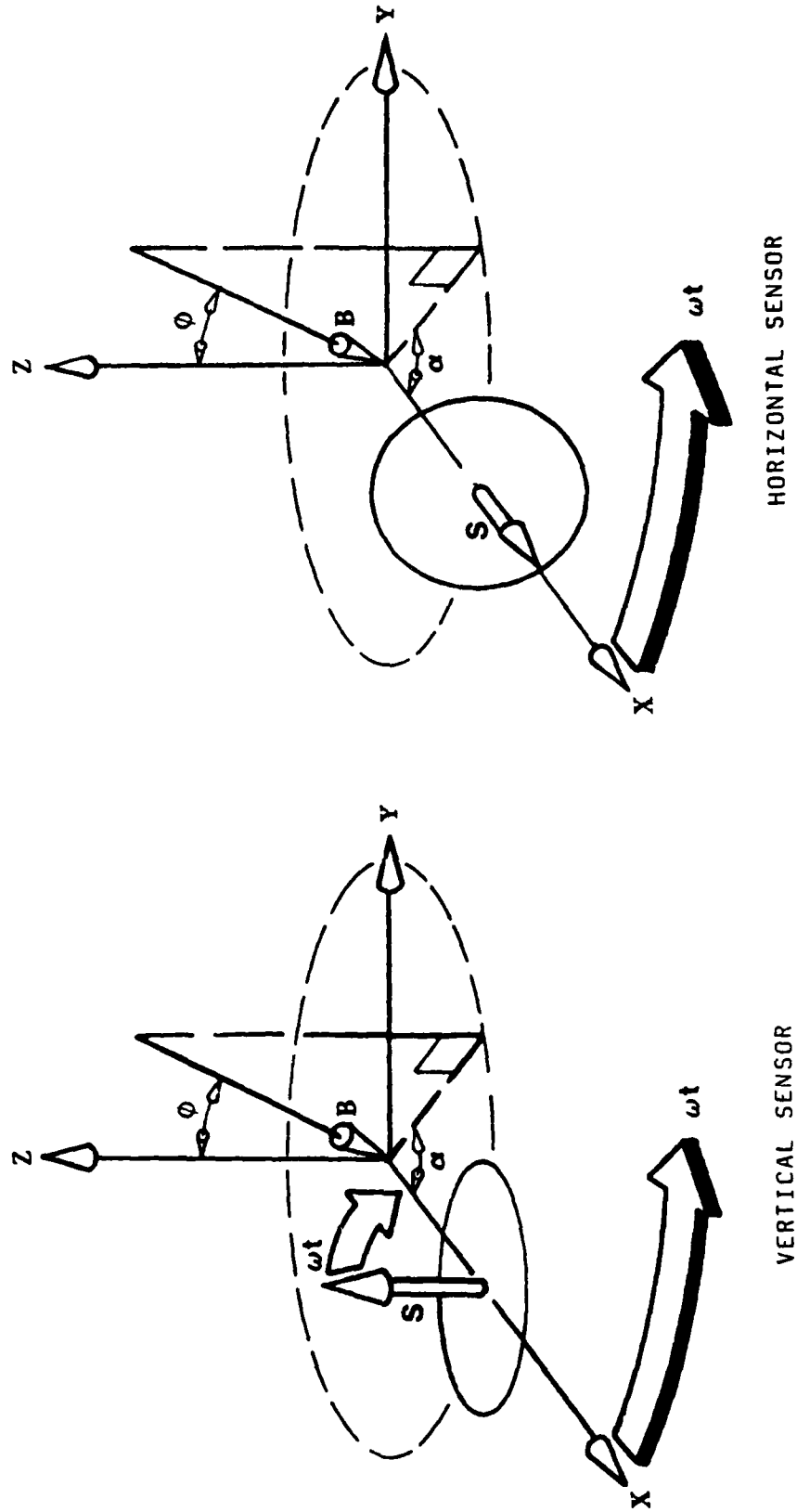
Figure 7. Cycloidal Magnetic Vector Sensor

22

5.2 DRIVING MECHANISM

Two basic driver mechanisms which could generate the desired motion were considered intially. These were an active drive mechanism where the rotational force can be directly transmitted to the sensor coil by bevel gears or an equivalent mechanism, and a passive system whose transmission can be performed by a flexible cable without any gear arrangement. An active driver mechanism was preferred and implemented in this design effort. The potential problems with the passive mechanism are:

(a) It is difficult to maintain a constant angular velocity of the sensing coils.

(b) It is difficult to implement dynamic balancing of the rotating members.

(c) The probability of a shorter life span of the mechanism due to failure of the flexible cable.

Two sets of bevel gears is a better choice than the single set of bevel gears used in the original FGL breadboard. Radial unbalance can be eliminated by two sets of gears, and two sets have a better synchronous noise capability as far as radial field distortion is concerned. Figure 6 shows the cut-out view of the two sets of bevel gear drive mechanism. The two sets of gears are separated such that they meet the rotational requirement of untwisting the wires connecting the gears. This arrangement does not satisfy all the balancing requirements, only the radial balance.

A DC motor was attached to the shaft to provide the rotational driving force.

5.3 ELECTRICAL WIRING BETWEEN THE SENSING COILS AND THE CASE

The most important factor in the design of the CMVS is the wiring that connects the rotating coils to the frame. This wiring takes the place of slip rings. The flexible wires from the coil assembly to the frame must be durable so that they can rotate for a large number of cycles. The mean-time-between-failure goal is 1000 hours. This goal can be achieved by constructing connecting wires similar to a telephone receiver cable where

23

flexible electrical conductors are used in a coiled form. The telephone
cable type conductor, which is a metal foil, was not suitable. After some in-
vestigation, a medical application type of conductor, size CZ1174, Cat. No.
9705, made by Cooner, proved suitable. This conductor is Teflon coated bio-
flex wire, size #36, made of 25 strands of #50 size wire. Sixty-five million
(65,000,000) rotations in test did not fail this wire. These tests indicated
that any other motion than the necessary rotational flexing is the main cause
of breakage of the wire. This can be prevented by restraining the wire
motion. Therefore, the width of the wire guide is important, as well as its
radius. It is the author's belief, and tests to date indicate, that the
flexing of the wire connecting the coils to the frame will not be a problem
in applying the CMVS, and the mean-time-between failure will be acceptable.

5.4 SENSING COIL ASSEMBLY DESIGN

The basic requirement in designing the coil assembly is to have the
maximum number of turns within the allowable area encircled by the coil, and
still provide for easy fabrication. The assembly shown in Figure 7 met the
necessary criteria. For this type of coil, a self supporting or bonded rigid
coil irregular in shape, is required. For this purpose, wire is used with a
base coat of conventional enamels, to obtain basic properties, and topped with
one or two coats of a thermoplastic bondable overcoat. In use, the wire is
wound into a coil, held in the required form, heated to the specified temper-
ature and allowed to cool. The bondable overcoat softens at this temperature
and upon cooling will be sufficiently bonded to make a rigid coil. The coils
each consist of 12,000 turns of Viking P-Bond #1 wire. The primary insulation
is polyurethane with a thermoplastic overcoat based on polyvinyl butyral
resin. This coating is thermoplastic at approximately 135°C. This wire is
made by MWS Precision Wire, 20731 Marilla St., Chatsworth, CA 91311. Tooling
was made to wind these coils. With the tooling, the coils were not difficult
to fabricate.

5.5 BEARINGS

It was decided to use ball bearings rather than bushings between
the rotating mechanism and the case. Possible problems with thermal expansion
coefficients and the stiffness of a bushing made the ball bearing a more

24

attractive possibility. However, it was not possible to find a commercially available bearing made of nonmagnetic material. Therefore, a standard commercially available bearing made of 52100 C stainless steel was used which is magnetic. It appeared from the test data that the magnetic properties of the ball bearing was causing come bias scattering depending on the input angle of the magnetic field. In a future build, a lubricated nonmagnetic bushing should be tried. It was also discovered that the bearing outer race must be fastened to the case or the repeatability of bias is affected.

5.6   POSITION REFERENCE SIGNAL

Equation 4-1 in Section 4.3 shows the absolute angular position of the rotor can be calculated accurately without a reference. However, an optical position indicator was added for test. The rotating part of the optical position indicator is a disc (in this design a planary gear was used) with 9 holes in it. Eight of the holes are placed in a circle with a 45 degree angle between them. These holes are used to locate the position of the rotor. The other (ninth) hole is used to count the revolutions, and is placed on the same circle as the other eight and halfway between two of them. An optical detector and a Light Emitting Diode (LED) are placed one on each side of the disc, and on the same radius as the circle formed by the holes. As the holes pass in front of the LED, an optical path is formed with the detector. A set screw was designed into the disc so that its position could be adjusted to the shaft as required.

SECTION VI

THREE AXES VIBRATING ACCELEROMETER ELECTRONICS

6.1 ELECTRONIC OPERATION

The major requirement of the electronics is to operate the beams
at their fundamental vibration frequencies. When a beam is driven by an
electromagnetic field, the beam will oscillate at twice the electromagnetic
drive frequency. This is because the force generated is a squared function
of the applied magnetic field. Consequently, if the input current to the
coil is a sine function, the force applied to the beam will be at twice the
frequency of the input sine wave. The method chosen to maintain the beam
oscillation at the same frequency as the drive current is to add an offset
(bias) to the driving flux. This can be explained in the following manner:

$$F = B^2 K \qquad (6-1)$$

where

  F   is the force applied to the beam

  B   is the magnetic flux applied

  K   is a constant

If the driving current is sinusoidal, i.e., $B = (\sin wt)$, then

$$F' = (C \sin wt)^2 K$$

$$= C^2 \sin^2 wt \ K \qquad (6-2)$$

The beam oscillates at twice the frequency of the input current.
If a bias A is added, however

$$F = (A + C \sin wt)^2 K$$

$$= (A^2 + 2\ AC \sin wt + C^2 \sin^2 wt)\ K$$

$$= 2\ AC\ K \sin wt + K\ A^2 + KC^2 \sin^2 wt \qquad (6-3)$$

26

Now, if the beam is driven so that the input frequency is the same as the beam resonance, then the beam will operate at the same frequency as the input. This flux bias eliminat... the need for frequency division in the oscillation loop.

When the input (drive) frequency is at the fundamental resonance (first harmonic) of the beam, then the third term in Equation 6-3 is eliminated.

The second term in Equation 6-3 (KA^2) is a DC force that is applied by the electronics to control the beam tension. The "coarse" tension is adjusted mechanically as described in Section 3.2, then the "fine" tension adjustment is applied by electrically varying the magnetic flux that drives the beam. This flux bias performs the following functions:

(a) Makes it possible to operate the beam at its fundamental frequency.

(b) Eliminates the scale factor non-linearity and bias shifts described in Section 3.2.

(c) Allows for finer setting of the oscillation frequency of the beam than is possible by mechanical tension adjustment.

6.2   CIRCUIT DESIGN

The flux bias is generated by applying a DC voltage to the driver coil. A method of applying the bias is shown in the schematic, Figure 8. The outputs of the tuning circuits from both outputs of one axis are applied to the D/A to generate a voltage B. B is proportional to the combination of the frequencies from both axis ($f_1 + f_2$). B is now applied to a sample and hold circuit (AD582) which is latched by the control signal C, supplied from the 8205. The voltage is applied through the LM318 amplifier. The advantage to applying the bias as a function of both beam frequencies of an axis is that the bias will vary in such a manner as to cause both beams to track each other, linearizing the scale factor and eliminating temperature and aging bias change effects. This circuit will also allow fine trimming of the frequencies of the beams (by selection of the gain resistor at the drive stage) so that each beam can be driven at a unique frequency, which is the fine adjustment to eliminate "frequency lock". The magnetic reluctance between the beam and the coil changes as a function of the beam vibration.

27
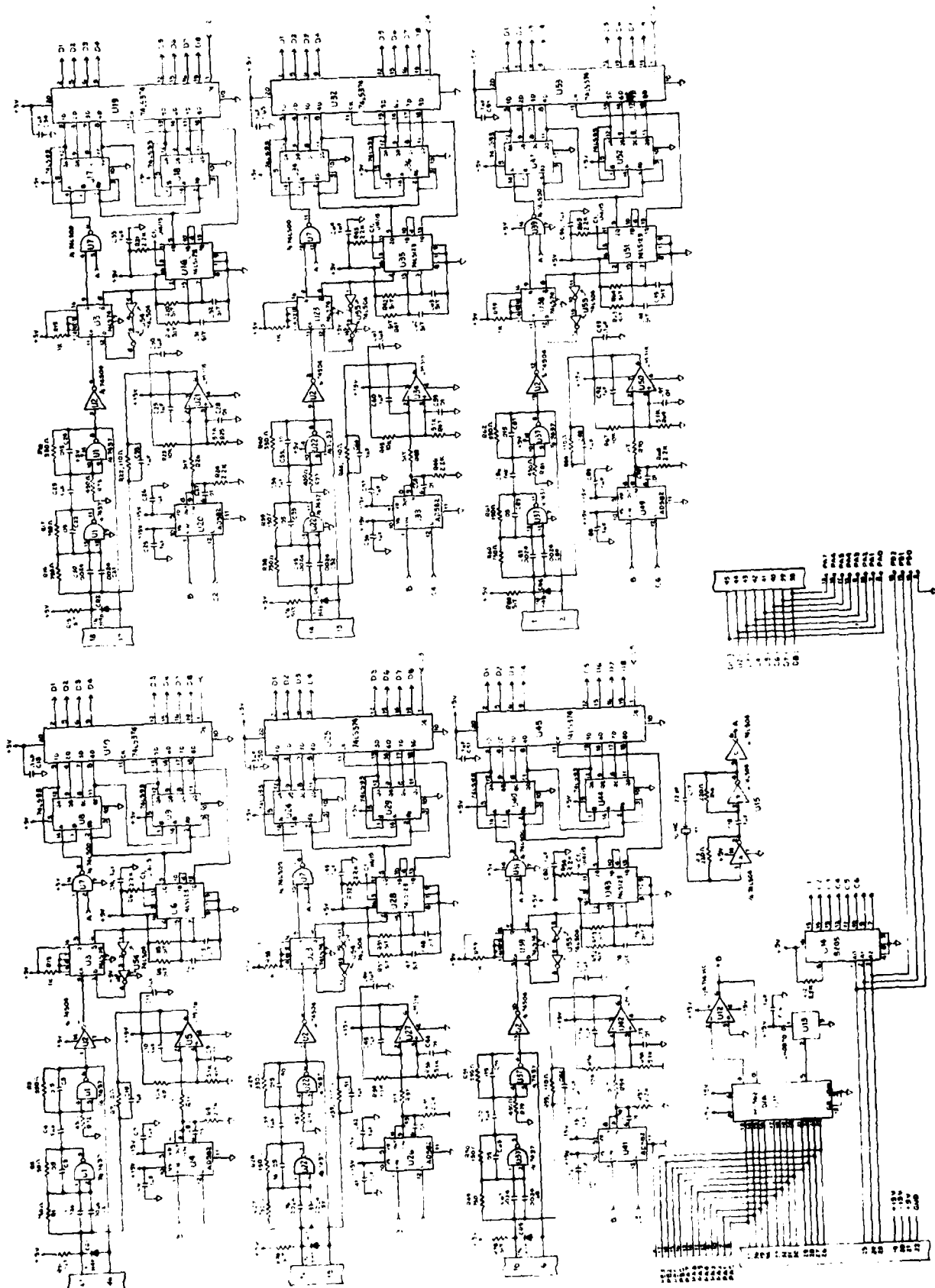
Figure 8. Three Axis Accelerometer Schematic

This changing reluctance can be used to control the beam driver circuit such that the circuit frequency is directly coupled to the beam oscillation. A positive feedback circuit, with the beam in the feedback loop, has been developed.

Two TTL inverters are configured as noninverting amplifiers and the electromagnetic coil closes the feedback loop. One of the TTL family of circuits, a 7437, has been chosen because of its current capability of 40 mA. One 7437 can drive an axis (both beams). Three of the 7437's provide all the necessary driver amplifier circuits. Since the TTL operates as a square wave, a damping diode across the driver coil is necessary to suppress inductive feedback. The output frequency of this oscillator is buffered by a Schmitt Trigger inverter and is divided in half to obtain the precise time period of the oscillation. The time interval is measured by a gated clock frequency which is generated by a crystal. Each period of the interval is stored in a data latch network 74LS374. The 74LS374 can latch 8 bit to 255 counts. To avoid overflow in the counter and latch circuit, a maximum of 6000 x 256 = 1,666,000 Hz can be used for the clock frequency. A higher clock frequency is desirable to improve the resolution but this will overflow the counter and latch. To improve the resolution, a clock of 10 MHz was tried. However, now the counters overflowed. To resolve this without going to a 16-bit interface, the difference in the periods of the outputs was measured, according to the following equation:

$$f_1 - f_2 \cong \frac{2}{T_1^3} \ (\Delta T_1 - \Delta T_2)$$

where ΔT_1 and ΔT_2 is the remainder after the overflow of T_1. The T_1^3 term is considered a part of the scale factor and can be established by the calibration procedure.

SECTION VII

CYCLOIDAL MAGNETIC VECTOR SENSOR ELECTRONICS

7.1   GENERAL DESCRIPTION

Four methods of processing the magnetic sensor signals were con-
sidered. The considered methods were phase detection, analog decoding,
digital processing or a calibration of one of the previous three. The
analog decoding method was used because it is a simple circuit that provides
vector information instead of only angle. Also all three axis of data can
be obtained from a single set of vertical coils and digitizing of the signals
can be implemented without a high throughput requirement. The block diagram,
Figure 9, shows the input signal out of the vertical pair of sensor coils
is buffered and amplified to obtain approximately a 5V P-P signal. This
amplified signal is fed to a switching integrator whose function will be
described in greater detail later. The signal generated by the optical
position indicator, described in Section 5.6, and which is located on the
magnetic sensor is processed so that accurate rotor position information will
be known. This position signal is utilized to generate the reference signals
required for the quadratic detector scheme. The desired signals for the X
and Y axes are at twice the spin speed (2N). However, the signal generated
at the spin speed (1N) is passed through by the demodulator. Two sample and
hold circuits are used to eliminate the fundamental (1N) frequency but main-
tain the 2N signal. The required signal for the Z axis measurement is at 1N,
so the demodulator is operated at a bandwidth which eliminates the 2N, and
only a single sample and hold circuit is needed.

7.2   AMPLIFIER STAGE

Referring to the schematic (Figure 10), jumper board JR1 is
provided to select the right combination of sensor signals. The polarity of
the signal is chosen such that two signals from the pair of vertical coils
can be arithmetically added. This added signal is connected to differential
input buffer amplifier uA714. The next stage amplifier, LM318, has a gain of
approximately 25. It has a 0.033 µF filter capacitor in the feedback to
suppress high frequency noise. The output of amplifier LM318 is branched into
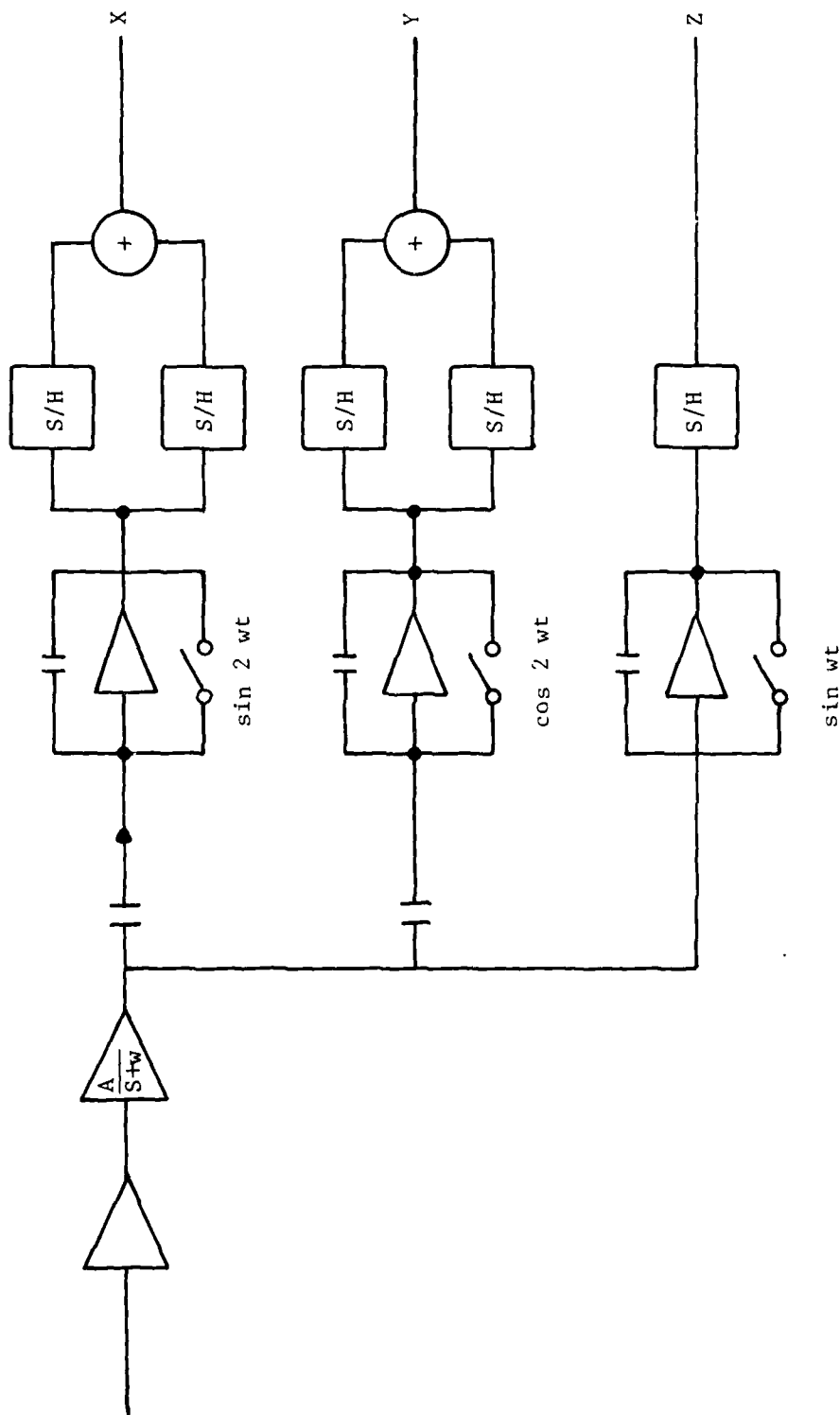three separate circuits which generate the X, Y and Z signals, respectively.

30

Figure 9. Block Diagram of Magnetic Sensor Decoding Electronics

31
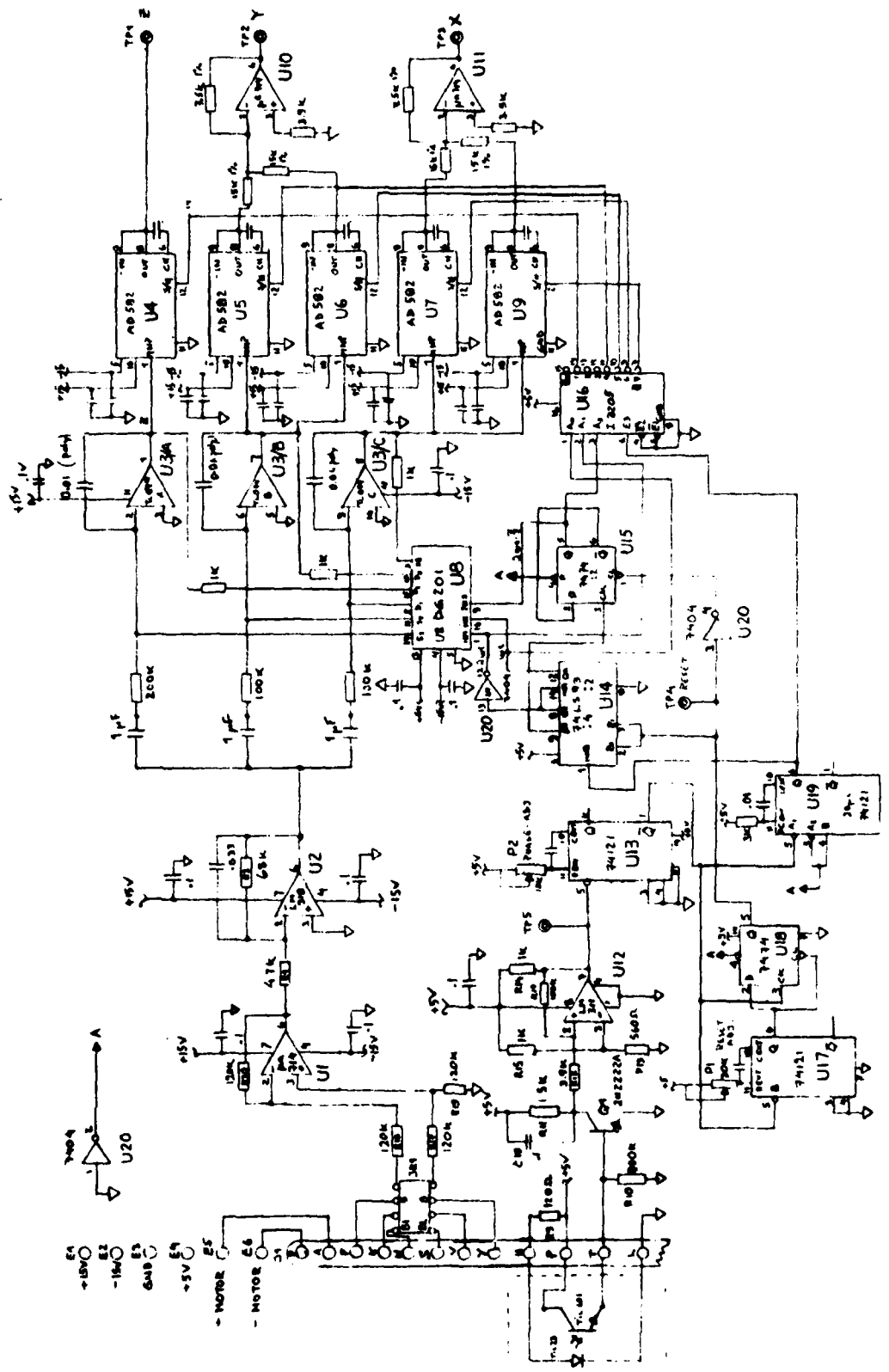
Figure 10. Cycloidal Magnetic Vector Sensor Schematic

7.3   SWITCHING INTEGRATOR

Three basic functions are performed in the switching integrator:

(a)   Reduction of the angular velocity dependent terms of the signal.

(b)   Serve as a quadratic demodulator.

(c)   Reduce high frequency noise.

This switching integrator consists of a Miller type integrator with a capacitor discharge MOS switch. The switch opens at the 0° and 180° positions of the demodulation reference signal. This allows integration of the input signal. When the output reaches the final level, the sample and hold circuits sample the integrator signals. For the rest of the period of the reference signal (i.e., 180° to 360°), the switch remains closed which discharges the integrating capacitor such that the output of the integrator stays at zero. **Figure 11** shows the relative time sequence of the integration and sample and hold circuit control signals.

7.4   DEMODULATION REFERENCE SIGNAL

The rest of the circuitry shown in the schematic is dedicated to the generation of the demodulation reference signals and sample and hold control signals. The LED and detection diode are mounted on the magnetic sensor as described in Section 5.6. Q_1 (2N2222A) amplifies the switched optical signal, and the voltage at the collector of Q_1 is further compared with a zero voltage reference to nerate a low noise square wave signal at the output of the LM311. There are 8 position signals spaced at 45° generated by the optical sensor/hole combination. There is also a ninth hole set at 22.5^O between two of the eight. This hole is designated as the reference for the other eight. The separation of the reference from the other eight positions is performed by a fixed time comparison technique achieved by the 74121 and 7474 components. The combination of the reference signal and the eight position signals generates the required demodulation references for the three demodulators. These signals are generated by a countdown performed in the 74LS93 and 7474. A three-line to eight-line decoder, 3205, is used to generate the sample and hold control signals.
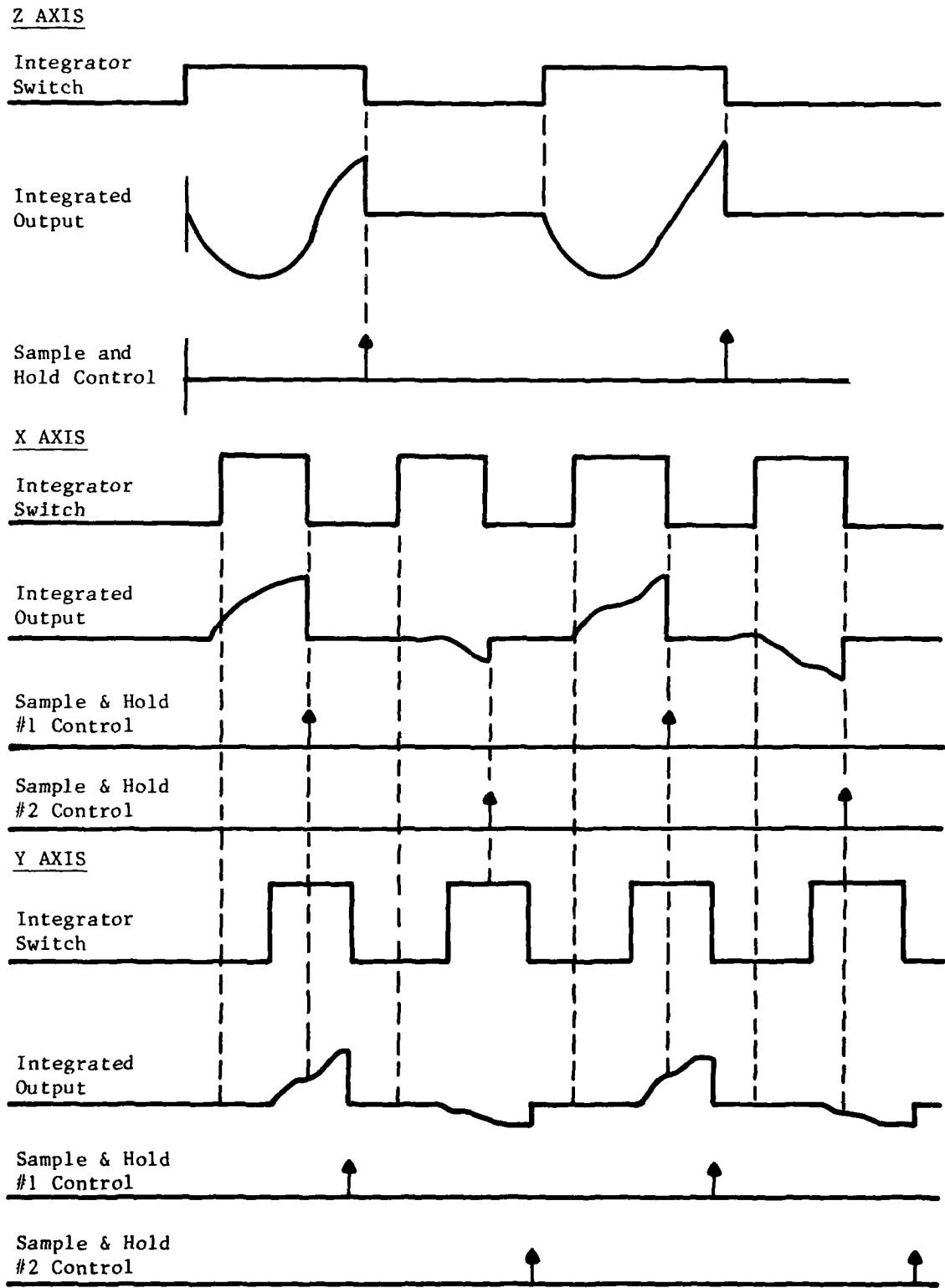
Figure 11. Timing Sequence for the 3-Axis of
Magnetic Sensor Electronics

34

SECTION VIII

CYCLOIDAL MAGNETIC VECTOR SENSOR TESTS

8.1   INTRODUCTION

The objective of the tests is to define performance parameters for airborne applications of the Cycloidal Magnetic Vector Sensor. The primary application of the sensor is to detect orientation angles of the magnetic vector with respect to the earth's magnetic field. To do this, the field measurement range, and noise sensitivity characteristics of the sensor is important. Also, the scale factor and axis alignment between three primary axes must be well defined during sensor calibration. Secondary factors for the sensor application are linearity, repeatability, and response time. One of the important factors that was evaluated during the testing was electromagnetic interference from the driver motor which can distort the earth's magnetic field. Preliminary study showed the location of the driver motor relative to the sensor axes introduces errors in linearity and axis alignment. This error was evaluated during the testing.

8.2   TEST EQUIPMENT AND FIXTURING

The objective of the laboratory test equipment is to produce realistic environmental conditions for each parameter under test.

8.2.1   Magnetic Field Generator

The primary reference laboratory magnetic field generator is a Helmholtz coil used to simulate uniform magnetic fields of sufficient strength where the sensor is located. The field strength is 0 to 1 gauss with a capability of changing the field in 10 milligauss steps. A 3-axis Helmholtz coil was constructed to meet these requirements. This consists of three sets of coils mounted orthogonally to each other. Figure 12 shows the 3-axis Helmholtz coil. Each axis of magnetic field can be adjusted by changing the applied current to each coil set. Even though this field generation does not produce a uniform field around the center, it is convenient to change the field strength. Also the angles (heading angle α and inclination angle ϕ) can be changed by varying the current to two sets of coils simultaneously.
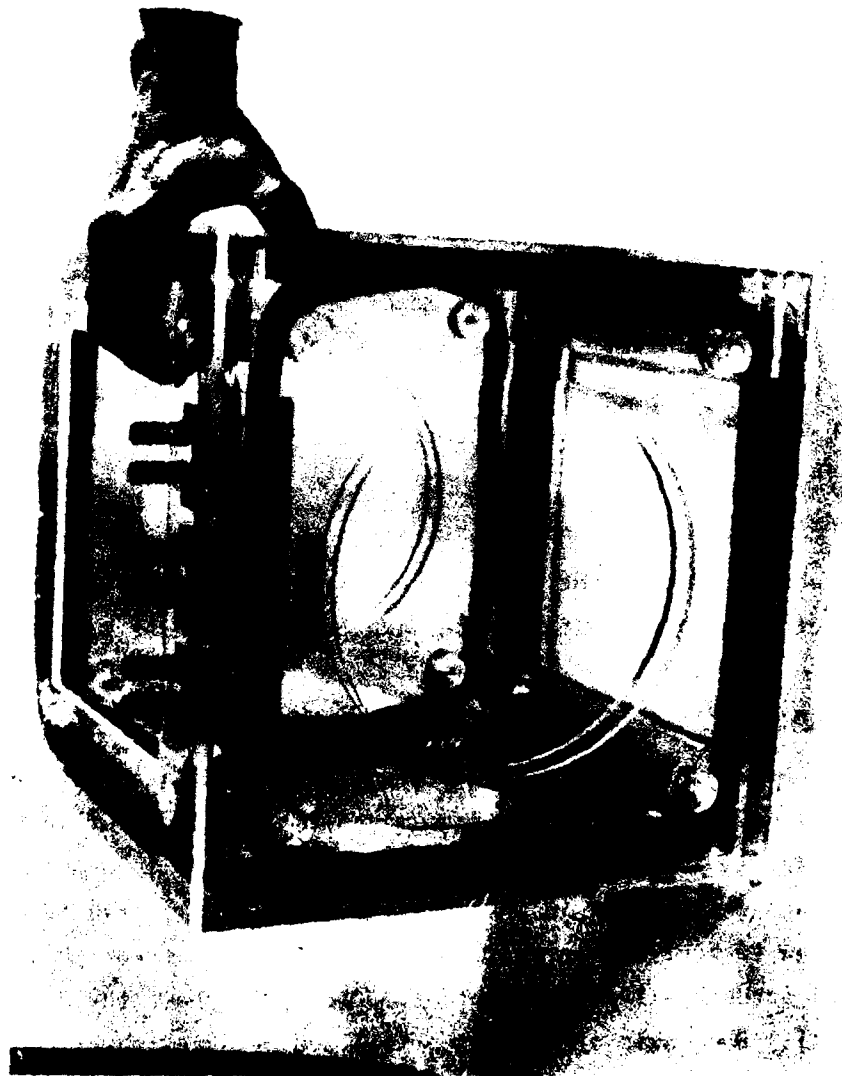
Figure 12. Helmholtz Coil

8.2.2   Indexing Head

The indexing head provides accurate orientation of the sensor with respect to the magnetic field. The indexing head is made from non-magnetic material so that the earth's magnetic field is not distorted. The resolution of the indexing head is better than 0.1 degree absolute.

8.2.3   Sensor Mounting Fixture

Hardware of a non-magnetic material was used to mount the sensor on the indexing head and to place the sensor in the Helmholtz coil field. Figure 13 shows the set-up used in the tests. The sensor mounting fixture and indexing head are shown with the CMVS inside the Helmholtz coil.

8.3   CALIBRATION

Initial calibration of the magnetic sensor has to be performed for accurate performance. Calibration is to:

    (a)   establish the sensor coil orientations,

    (b)   establish the alpha angle with respect to the case,

    (c)   define the optical position reference signal with respect
          to the case,

    (d)   determine the coherent magnetic field distortion.

Two sets consisting of two coils each are mounted on the sensor rotor. Two are for vertical sensing and two are for horizontal sensing. Sensing coils on opposite sides are connected such that the signal from each coil is additive. The phase relationship between the horizontal and vertical signals are as described in equation 4-1 for CCW rotation of the rotor. An oscilloscope was used to monitor both signals and to determine their relationship. The rotor axes orientation with respect to the case is also established at the same time. When the vertical coil area vector is parallel to the rotation (Z) axis of the CMVS, then the line which lies along the rotor arm, that supports the coil, is the X axis of the instrument. The Y axis is orthogonal to the X and Z axes. These axes are only defined at this stage, as the axis alignment is performed later.

Figure 13. CMVS Test Set-Up

38

The preferred way of adjusting the optical wheel position reference with respect to the case is to monitor the output signal of the electronics. The position reference signal is used to reset the integrator and counter logic in the electronics. The phase relationship between the position reference signal and the signal output from the sensor coils determines the relationship between the Alpha and Phi angles. The wheel position with respect to the rotor can be adjusted by adjustment of the set screw on the wheel. An oscilloscope trace of the coils is used to reveal any unnecessary field distortion in the instrument, caused by magnetic materials used in constructing the instrument or test fixtures. Any unnecessary magnetic material in the vicinity of the CMVS was eliminated.

8.4   LINEARITY

Linearity was measured by changing the indexing head set angle and reading the heading angle (α) indicated by the CMVS. Figure 14 shows both heading and inclination angles. The measured linearity of the heading angle falls within the spread of accuracy of the instrument. This is shown by the fact that the inclination angle, which is not being rotated and therefore can have no nonlinearity, has the same error spread as the heading angle, which is being rotated. Further investigation indicated the majority of the error is due to the position of the bearings as they are rotated with respect to the coils. The bearings are standard ball bearings which have sufficient magnetic properties to distort the magnetic field.

8.5   AXIS ALIGNMENT

Figure 15 shows the relationship between α (heading) and ϕ (attitude) of the sensor axes. The optical reference wheel is installed initially with an arbitrary orientation to the sensor axes. To align the axes an input is applied along the X axis from the Helmholtz coil, and the output from the Z axis is measured. The X axis is now inclined until the Z axis output suddenly changes from 0 to 180 degrees. Figure 15 shows that this point occurred at 29.3 degrees of X axis inclination for the particular CMVS under test. This means that the optical reference wheel needs to be rotered by 29.3 degrees. The set screw in the optical reference wheel is now loosened, and the wheel rotated by the required angle. This aligns the CMVS

Figure 14. Heading (α) and Inclination (ϕ) Angle Errors

Figure 15.   Relation Between α and φ Angles

axes. The observed change of the axes orientation after the alignment correction was performed was not significant compared to the sensor resolution.

8.6 FIELD MEASUREMENT RANGE

Test showed that the effective measurement range of the CMVS is a maximum of approximately 2 Gauss and a minimum of approximately 0.05 Gauss. The maximum is not limited by the sensor but by saturation of the electronics. The minimum appears to be limited by sensor noise. The signal-to-noise ratio can be improved by increasing the spin frequency of the sensor.

8.7 REPEATABILITY

Repeatability was observed to be 0.27 degrees 1 sigma. It was measured by turning the CMVS on and off 12 times, and reading the measured angles. The results are shown below:

Trial Number	Measured Angle - Degrees
1	29.5
2	29.7
3	29.9
4	29.1
5	29.5
6	29.0
7	29.4
8	29.1
9	29.2
10	29.4
11	29.7
12	29.5
Mean Angle	29.42
1 sigma Variation	0.27

8.8 DRIVER MOTOR INTERFERENCE

The ideal position of the drive motor, which can cause magnetic field distortion, was found to be on the spin axis of the spindle. It is apparent

that the further the motor is from the sensing coils the less distortion will result. The practical distance, however, is limited by the desired size of the CMVS package. Data shows that a 5 inch separation from the center of the spindle to the center of the motor was acceptable, and caused no significant errors.

SECTION IX
VIBRATING BEAM ACCELEROMETER TESTS

9.1   INTRODUCTION

It was discovered in trying to obtain data that the bias was un-
stable to such an extent that visibility of the characteristics of the
instrument was obscured. Investigation revealed the fact that beams of dif-
ferent thicknesses do not track each other, i.e., their changes in frequency
as a function of a change in beam tension are different. This causes an in-
stability of the bias because the tension changes as a function of temperature,
etc. The effect was described in Section III, and a solution suggested. The
solution to resolving the bias shifts, and linearizing the scale factor, by
dynamic compensation of the tension in the beam, was developed to the point
of including the necessary hardware. However, the implementation requires a
computer and software, and resources were not available to perform these
tasks under this contract.

Data was taken without the tension compensation, but the results
are affected, and sometimes totally obscured, by the unstable bias.

9.2   TEST METHODS

It was also discovered that the methods described in the test plan,
attached as Appendix A, were not sufficient to evaluate the accelerometer
performance. Computer aide is required to calculate the frequencies for each
vibrating beam, so that the difference frequency can be measured. After a
severe bias instability was discovered by using the methods described in the
test plan, a computer was introduced to analyze the accelerometer. The
computer was used to perform theoretical compensation of the beam tension.
Practical dynamic compensation by controlling the beam tension by varying the
driving force was not attempted.

As described in previous sections, it is necessary to generate soft-
ware to measure the beam tension, rather than just measuring frequency, such
that $T_1 - T_2$ is proportional to the acceleration. Meanwhile $T_1 + T_2$ can be
implemented to perform tension compensation. Figure 16 is a flow chart of a
recommended data handling routine.
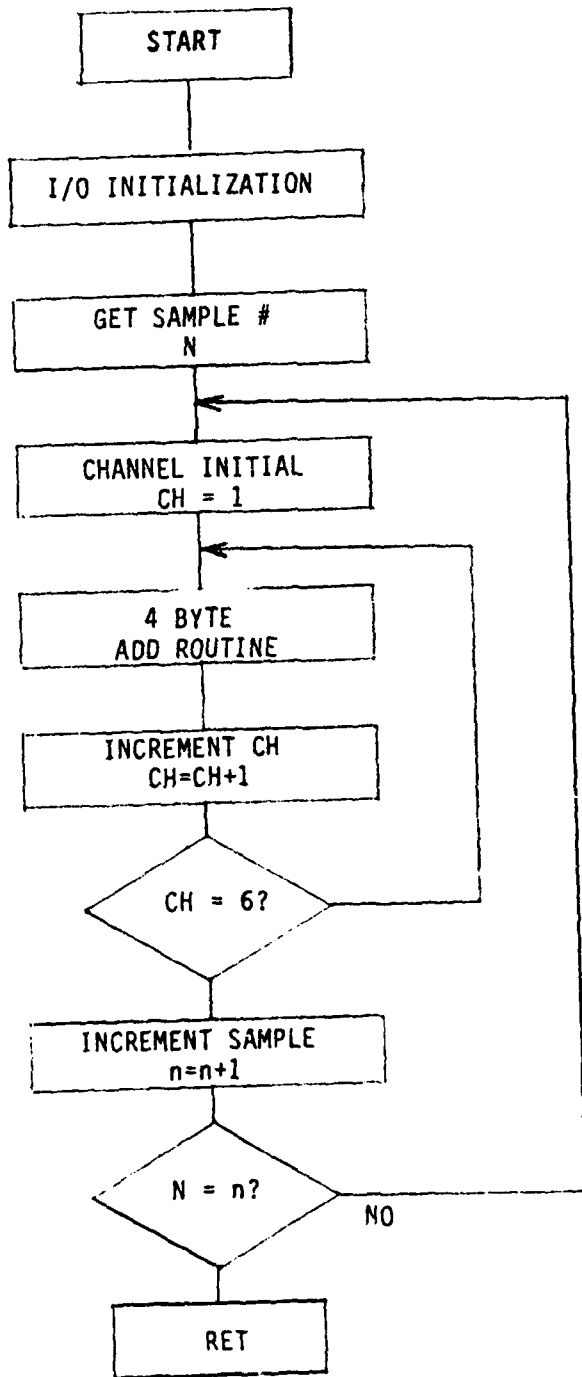
Figure 16. Assembler Language Flow Chart

The Intel 8080 Based Altair[R] computer assembly form is also attached. The assembly *form for the* computer language is recommended because the throughput required for handling data from six beams is significant. This assembly section performs:

(a) Select and scan the beams

(b) Read data

(c) Accumulate data for a given period

I/O handling is accomplished by an asynchronous technique, i.e., computer read data *is from a six channel counter* which is latched regardless of the beam frequencies.

Additional *tasks required to complete the* calculations are:

(a) Calculate the tension of each beam

(b) Calculate acceleration from $T_1 - T_2$

(c) Calculate the tension compensation from $T_1 + T_2$

(d) Transmit $T_1 + T_2$ to I/O

9.3 TEST RESULTS

	Goal	Measured
Random Bias Variation Drift (1 sigma)	1.5×10^{-4}	1.5×10^{-2}
Long Term (Day-to-Day) Bias Repeatability	1.5×10^{-3}	$1.0 \times 10^{-1}g$
Acceleration Sensitivity	$1.5 \times 10^{-3} g/g^2$	?
Scale Factor Accuracy	500 ppm	1,000 ppm
Non-Linearity	500 ppm	?
Symmetry/Asymmetry	50 ppm	?
Threshold	50 g	1 mg
Scale Factor	---	10 - 13 Hz/g

Due to the high instability of the bias, it was impossible from some tests to determine reasonable numbers. Measured random bias variation is approximately 15 mg, which obscures and distorts some of the other parameters.

TABLE I. COMPUTER ASSEMBLY LISTING

```
STRS

STRS

ASSM.TO
ERROR
ASCM+ .3000 7000

ASSM .7063 7000
7000              0000 *     3-AXIS ACCEL. FILE/AXIC3/ 03-06-81  H.1
7000              0010 IPA      EQU   0DF80H
7000              0020 CPA      EQU   0DF81H
7000              0030 OPB      EQU   0DF82H
7000              0040 CPB      EQU   0DF83H
7000              0050 CHID     EQU   7102H
7000              0060 SAMPLE   EQU   7100H
7000              0070 CLEAR    EQU   7217H
7000              0080 BUFFER   EQU   7200H
7000 01 81 DF     0090          LXI   B,CPA     ;INIT PIA'S
7003 3E 00        0100          MVI   A,00H
7005 02           0110          STAX  B
7006 01 83 DF     0120          LXI   B,CPB
7009 02           0130          STAX  B
700A 01 80 DF     0140          LXI   B,IPA     ;PIA A INPUT PORT
700D 02           0150          STAX  B
700E 01 82 DF     0160          LXI   B,OPB
7011 3E FF        0170          MVI   A,0FFH
7013 02           0180          STAX  B     ;PIA B OUTPUT PORT
7014 01 81 DF     0190          LXI   B,CPA
7017 3E 04        0200          MVI   A,04H
7019 02           0210          STAX  B
701A 01 83 DF     0220          LXI   B,CPB
701D 02           0230          STAX  B     ;PIA S NOW INIT
701E 21 17 72     0240          LXI   H,CLEAR   ;CLEAR BUFFERS
7021 3E 00        0250 LOOPCL   MVI   A,00H
7023 77           0260          MOV   M,A
7024 2D           0270          DCR   L
7025 F2 21 70     0280          JP    LOOPCL
7028 32 82 DF     0290          STA   OPB     ;CH01 ADDRESS
702B 2A 00 71     0300          LHLD  SAMPLE    ;GET SAMPLE N
702E EB           0310          XCHG  ;D>E
702F 21 00 72     0320 CONT     LXI   H,BUFFER    ;BUFFER INDEX
7032 3E 00        0330          MVI   A,00H
7034 32 02 71     0340 NEXT     STA   CHID    ;SAVE CH ID
7037 3A 80 DF     0350          LDA   IPA     ;GO AND GET THE DATA
703A 00           0360          NOP
703B 86           0370          ADD   M,A     ;1ST BYTE.
703C 77           0380          MOV   M,A
703D 2C           0390          INR   L
703E 3E 00        0400          MVI   A,00H
7040 8E           0410          ADC   M,A     ;2ND BYTE
7041 77           0420          MOV   M,A
7042 2C           0430          INR   L
7043 3E 00        0440          MVI   A,00H
7045 8E           0450          ADC   M,A     ;3RD BYTE
7046 77           0460          MOV   M,A
7047 2C           0470          INR   L
7048 3E 00        0480          MVI   A,00H
704A 8E           0490          ADC   M,A     ;4TH BYTE
704B 77           0500          MOV   M,A
704C 2C           0505          INR   L     ;NEXT CHANNEL
704D 3A 02 71     0510 FINISH   LDA   CHID    ;GET CHANNEL ID
7050 3C           0520          INR   A     ;NEXT CHANNEL
7051 FE 06        0530          CPI   06H     ;LAST CHANNEL?
7053 CA 5C 70     0540          JZ    DONE
7056 32 82 81     0550          STA   OPB     ;CHANGE CHANNEL
7059 C3 34 70     0560          JMP   NEXT    ;CONTINUE
705C 1B           0570 DONE     DCX   D     ;DECR SAMPLE REG
705D 3E 00        0580          MVI   A,00H     ;TEST REG D
705F BA           0590          CMP   D
7060 C2 2F 70     0600          JNZ   CONT    ;CONTINUE TO SAMPLE
7063 3E 00        0610          MVI   A,00H
7065 BB           0620          CMP   E
7066 C2 2F 70,    0630          JNZ   CONT    ;CONTINUE TO SAMPLE
7069 C9           0640          RET

+S .7000 725M
+S .7000 7250
```

47

SECTION X

CONCLUSIONS AND RECOMMENDATIONS

The Cycloidal Magnetic Vector Sensor is developed to the stage where it could be packaged for production. The packaging requirement is only for the electronics, which have not yet been incorporated as an integral part of the mechanical unit. To further improve the design the standard ball bearings, which have magnetic properties that affect the CMVS accuracy, could be replaced by a non-magnetic bearing. This will take some development because the new bearing will probably not be a standard, off-the-shelf bearing. The favorite candidate is a non-magnetic (possibly bronze) bushing.

The 3-Axis Vibrating Beam Accelerometer needs further development to be ready for navigation applications. It is **believed** that the incorporation of dynamic beam compensation, i.e., controlling beam tension so that the algebraic total is constant at all times, would greatly improve performance. The fundamental ideas of using the concept described in this report does appear to be feasible, and would result in a low cost accelerometer.

APPENDIX

T E S T   P L A N S

A.   THREE AXIS VIBRATING ACCELEROMETER

B.   CYCLOIDAL MAGNETIC SENSOR

December 31, 1979

INCOSYM, INC.
780 Lakefield Road
Westlake Village, CA 91361

A. THREE AXIS VIBRATING ACCELEROMETER

1.0 INTRODUCTION

*The objective of the following is to provide a detailed test plan for
approval by the Air Force prior to the beginning of the test phase.
The objective of the tests described is to determine the potential of
the three-axis accelerometer to accomplish the design goals required
of a low-cost RPV (Remotely Piloted Vehicle).*

2.0 DESCRIPTION OF TEST ITEM

The unit to be tested is a low-cost, three-axis, open loop vibrating
beam accelerometer (C3VB) with a unique, single inertial mass. The
beam excitation and displacement pickoff utilizes a clever positive
feedback oscillation technique which provides an inherent digital
output. The sample tested is 3 x 3 x 3 inches and is mounted with
three mounting pads with bolt holes. The three output axes are desig-
nated X, Y and Z, and are mutually orthogonal with the Z axis perpen-
dicular to the mounting surface.

The supporting electronics, which provide beam excitation and displace-
ment measurement, is contained in a 6 x 8 x 12 nch electronic box.
The box will also contain processing circuitry for the three-axis
digital readout.

2.1 Performance Goals

2.1.1	Random Bias Variation Drift (1σ)	1.5×10^{-4} g
2.1.2	Long Term (Day-to-Day) Bias Repeatability	1.5×10^{-3} g
2.1.3	Acceleration Sensitivity	1.5×10^{-3} g/g^2
2.1.4	Scale Factor Accuracy	

2.1.4.1	Long Term (Day-to-Day) Stability	500 ppm
2.1.4.2	Non-Linearity	500 ppm
2.1.4.3	Symmetry/Asymmetry	50 ppm
2.1.4.4	Threshold	50 μg

2.1.5	Physical Size (approximately)	50 cu. in. exclusive of electronics
2.1.6	Weight	< 3 lbs.
2.1.7	*Power Requirements*	< 2 watts
2.1.8	Dynamic Range	± 12 g

3.0 DESCRIPTION OF TESTS

The tests and test sequence prescribed are designed to determine if each sensitive axis of the C3VB meets the performance goals of paragraph 2.1. Tests will be performed on a dividing head or a precision granite cube containing a temperature controlled environment. A general description of the methods, the intended test sequence, and a detailed description of the individual tests are presented in the following sections.

3.1 Test Methods

For most tests, a HP-5280A Reversible Counter will be used to measure the output from a given axis. The Accelerometer Sense Electronics is shown in Figure 1, two of which are required per axis. Unless specified otherwise, all tests will be conducted with the three axis accelerometer maintained at 86^OF. (± 1^OF.) by using a closed loop temperature control. The electronic box containing the processing circuits will be at room temperature. The tests are to establish the basic performance characteristics of each sensitive axis in a zero and one gravity (g) field, and to determine the effects of time, temperature and voltage on these characteristics. The dividing head is manufactured by Vinco Corporation, Detroit, Michigan (Model 55-175) and has a temperature controlled oven incorporated in the assembly. The angular positioning accuracy is less than 10 arcseconds. Its horizontal axis is mounted and the maintained level is within ± 10 arcseconds. A spirit level, accurate to 3 arcseconds, is available to verify the level accuracy of the fixture.
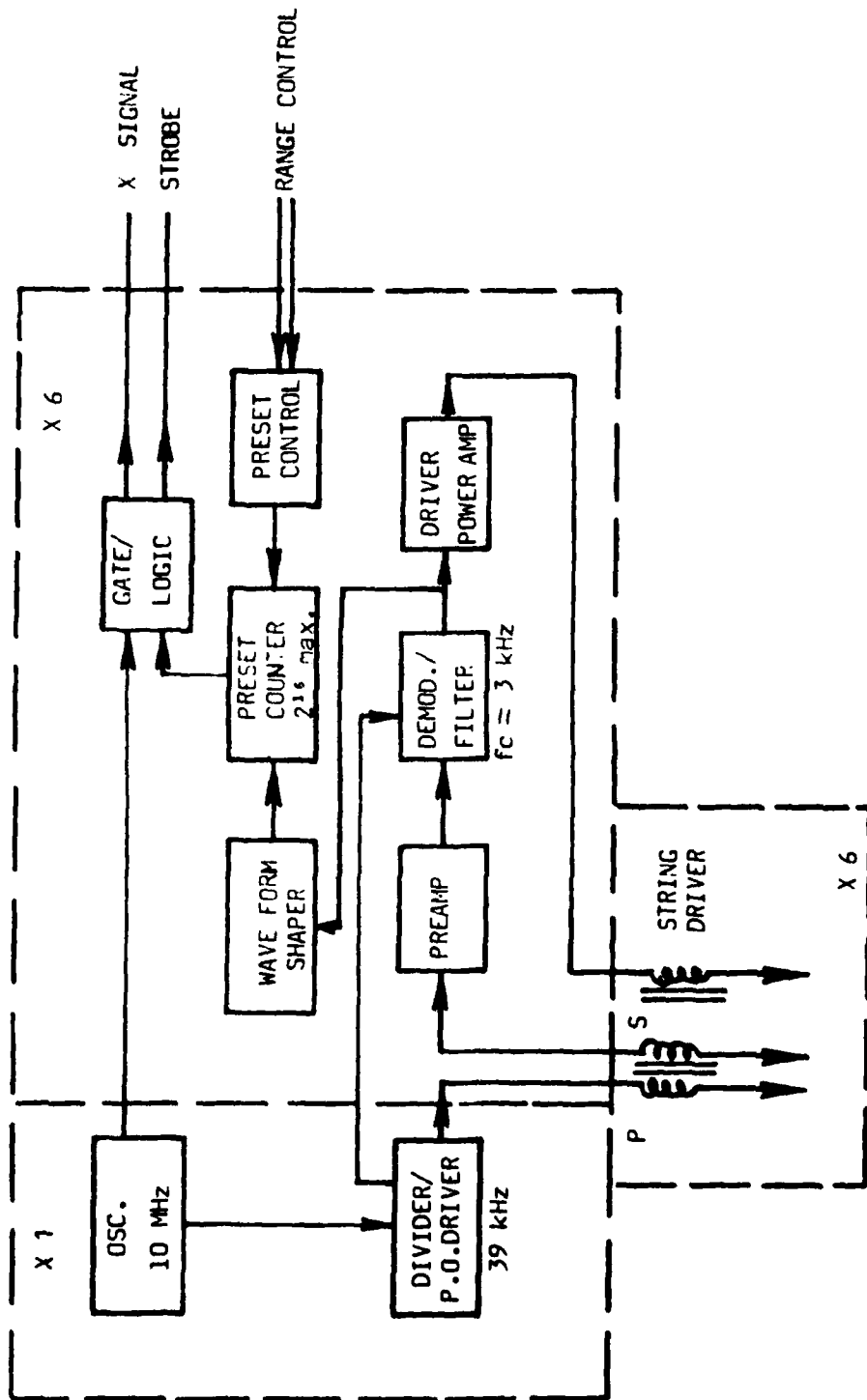
Figure 1. Accelerometer Sense Electronics

53

3.2   Test Sequence

The sequence of tests described below will be performed on each sensitive axis of the three-axis accelerometer. Some tests, particularly the temperature sensitivity tests, are repeated during the test phase to determine the effects of time and environment changes on the operating characteristics of the C3VB. The sequence of tests are:

3.2.1   Four Point (4 Pt.) Checkout

3.2.2   Warm-Up Time and Reorientation Settling Time

3.2.3   One Hour Stability and Random Bias Drift

3.2.4   Linearity

3.2.5   Threshold and Resolution

3.2.6   Narrow Range ($\pm$ 10°F.) Temperature Sensitivity

3.2.7   Repeat item 3.2.6 above

Some portions of the test sequence may be repeated if evaluation of the results are uncertain or anomalies are indicated.

3.3   Test Details

All of the following tests refer to evaluating the I_{AX}. Each test will be repeated to evaluate I_{AY} and I_{AZ}.

3.3.1   Four Point (4 Pt.) Checkout

This test is performed with the accelerometer mounted on the DH with its X input axis (I_{AX}) perpendicular to the axis of rotation of the DH and with the I_{AX} horizontal (both within one arcminute); this is the 0° reference position. The Y input axis (I_{AY}) of the accelerometer will be parallel to the DH axis of rotation. With the I_{AX} properly aligned, the DH will be rotated 90° to place the I_{AX} vertical. Data from the X axis will be recorded at this position, then the DH will be rotated in 90 degree steps in the sequence shown in Figure 2. Data will be recorded at each position for a total of five points. The data will be analyzed using the data reduction form shown in Figure 3.

54
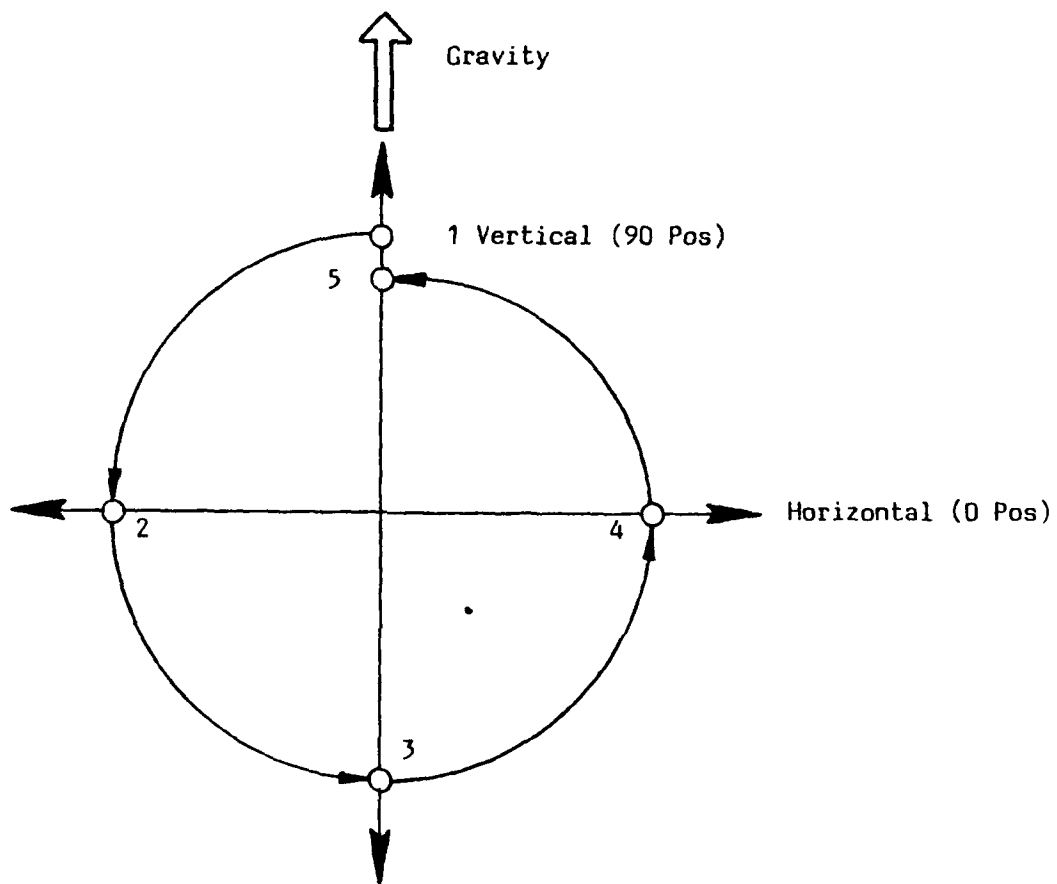
Figure 2.   Four-Point Test Sequence

C3VB DATA SHEET FOR 4 POINT TEST

Date_____   Accelerometer S/N_____   Operator_____

Temperature _____

POSITION	X_n	Y_n	Z_n
1			
2			
3			
4			
5			

SCALE FACTOR: g per counts per second

$K = \dfrac{2}{③ - ①}$			

BIAS: g

$B = \dfrac{① + ② + ③ + ④}{4}$			

Figure 3. Data Reduction Form

3.3.2 Warm-Up and Settling Time

The accelerometer will be placed on the DH with I_{AX} nominally vertical. Power will be applied to the unit and the mounting block (at room temperature) and the output of each axis sampled every five minutes including the accelerometer and block temperature. Data will be examined to determine the time required for the block to temperature stabilize, as well as the time at which the outputs first cease to exhibit a deterministic trend. With the accelerometer in the same position and block temperature stabilized, power will be turned off to the accelerometer (block heater on) for approximately one hour. Power will be reapplied and the output of each axis sampled every five minutes including the accelerometer temperature. Data will be examined to determine the accelerometer warm-up time.

3.3.3 One Hour Stability Test

The accelerometer will be placed on the DH and aligned preparatory to four point testing. Continuous 4 point testing will be performed at 10 minute intervals for one hour. The 4 point data will be examined to show stability of the performance coefficients over the one hour test period.

3.3.4 One G Linearity (Multipoint Test)

The accelerometer will be mounted on the DH, temperature stabilized, I_A aligned, and two 4 point tests performed. Starting with the I_A vertical, the DH will be rotated at 0.2 g increments for one complete revolution. Data will be recorded at each step and analyzed as described in paragraph 4.1. Two 4 point tests will be conducted immediately after the multipoint procedure.

3.3.5 Threshold and Resolution Test

With the accelerometer on the DH, the temperature will be stabilized, I_A aligned and two 4 point tests performed. The DH will be rotated to place the I_{AX} horizontal. The DH will be rotated to determine the approximate angle input where an output

is seen. The DH will then be rotated clockwise and counter-clockwise through this "dead zone" region in steps equal to 20% of the dead zone. The test will be repeated with I_{AX} at 30° above the horizontal, sensing positive g's. Two 4 point tests will then be done at the end of this sequence. The data will be analyzed as described in paragraph 4.2.

3.3.6 Narrow Range ($\pm 10^O$F.) Temperature Sensitivity Test

Four point tests will be performed at the normal operating temperature and with the I_A aligned. The instrument and blade temperature will be changed and stabilized and 4 point tests performed at the following temperature differences (^{O}F.): 0, +10, 0, -10, 0, +10, 0, -10 and 0. The resulting tempera-ture data will be analyzed as described in paragraph 4.3.

4.0 DATA ANALYSIS

4.1 Multipoint Test

A least squares straight line is used to solve for scale factors. The residuals from this fit are plotted and examined for indications of bias or scale factor asymmetry or nonlinear performance.

4.2 Threshold and Resolution Test

The output from the accelerometer will be plotted and the smallest amount of change in acceleration that can be sensed will be determined. The threshold (input axis starting at 0 g) and resolution (input axis starting at 0.5 g) will be determined.

4.3 Temperature Sensitivity Test

Accelerometer biases and scale factors will be obtained from 4 point tests conducted at various temperatures, using the procedures presented in paragraph 3.3.6. The values obtained will be plotted as functions of temperature. The bias and scale factor temperature coefficients will be obtained from a least squares fit of a straight line to the data. The temperature coefficient is defined to be the slope of the line. If the plots indicate, two slopes may be used to obtain temperature coefficients over the entire temperature operating range of the instrument.

B. CYCLOIDAL MAGNETIC SENSOR

1.0 INTRODUCTION

The objective of the following is to define performance parameters for airborne application of the magnetic vector sensor. The primary application of the sensor is to detect orientation angles of the magnetic vector sensor with respect to the earth's magnetic field. To do this, the field measurement range and sensitivity of the sensor is important as well as its noise characteristics. Scale factor (counts/deg) and axis alignment between three primary axes must be well defined for sensor calibration. Secondary factors for the sensor application specified in the work statement requires linearity, repeatability, and response time of the sensor.

One of the most important things to be evaluated is electromagnetic interference from the driver motor which may distort magnetic field where the sensor is sensitive. Preliminary study shows the location of the driver motor relative to the sensor axes introduces error in linearity and axis alignment of the sensor. This error will be characterized in the test.

2.0 TEST SET UP

Laboratory test set up should produce realistic environmental conditions for each parameter under test.

2.1 Magnetic Field Generator

The primary reference laboratory magnetic field generator will be a Helmholtz coil used to simulate uniform magnetic field of sufficient volume where the sensor is located. A pair of secondary coils may be required to improve uniformity of the field. The field strength should be 0 to 1 gauss with a capability of changing the field in 10 milligauss steps.

2.2 Indexing Head

The indexing head will provide accurate orientation of the sensor
with respect to the magnetic field. The indexing head should not disturb
the magnetic field unless its field distortion can be characterized. The
resolution of the indexing head should be better than 0.1 degree absolute.

2.3 Sensor Mount

Hardware of non-magnetic material is required to mount the sensor
on the indexing head and to place the sensor in the Helmholtz coil field.

3.0 *TESTS AND DATA REDUCTION*

3.1 Axis Alignment Measurement

1) Set magnetic field at 300 milligauss level

2) Perform data sheet 1 (Figure 1.)

3) Calculate:

$$\theta_{XZ} = \tfrac{1}{2}\left(\emptyset_X - \emptyset_{-X}\right)$$

$$\theta_{YZ} = \tfrac{1}{2}\left(\emptyset_Y - \emptyset_{-Y}\right)$$

3.2 Field Measurement Range

1) Orient X axis to North

2) Plot measured angle versus field strength

3) Repeat for Y axis and Z axis

4) By investigating the three plots, define field strength
   (B_{MIN}, B_{MAX}) and 1 sigma value of angle:

B_{MIN} α = _____ , $\emptyset$ = _____

B_{MAX} α = _____ , $\emptyset$ = _____

1 sigma α = _____ , $\emptyset$ = _____

3.3 Linearity Measurement

1) Measure and plot   versus set angle

2) Measure and plot $\emptyset$ versus set angle

3) Use quadratic curve fit technique and determine A_0, A_1, and A_2.

$$A_0 = \underline{\hspace{3cm}}$$

$$A_1 = \underline{\hspace{3cm}}$$

$$A_2 = \underline{\hspace{3cm}}$$

3.4 Repeatability Measurement

Set magnetic field at 300 milligauss and orient X-axis to N-E 45°.

1) Turn the sensor power on and off seven (7) times and
   record measured angle.

2) Calculate deviation 1σ value:

$$1\sigma \text{ on-off} = \underline{\hspace{3cm}}$$

3) Repeat 1) and 2) above for $\emptyset$ angle:

$$1\sigma \text{ on-off} = \underline{\hspace{3cm}}$$

3.5 Driver Motor Interference

1) By changing the position of the driver motor vertically in increments of 0.5 inch, repeat linearity test and document results.

2) By changing the position of motor horizontally in increments of 0.5 inch, repeat linearity test and document results.

3) Define best location of motor as far as the linearity is concerned.

4) Repeat 1) and 2) above, except change the motor position increments to 0.125 inch and document results.

DATA SHEET I

1. Orient sensor's X axis to North and measure α and $\emptyset$:

$$\alpha_X = \underline{\hspace{2cm}} \text{ degrees}$$

$$\emptyset_X = \underline{\hspace{2cm}} \text{ degrees}$$

2. Orient sensor's -X axis to North and measure α and $\emptyset$:

$$\alpha_{-X} = \underline{\hspace{2cm}} \text{ degrees}$$

$$\emptyset_{-X} = \underline{\hspace{2cm}} \text{ degrees}$$

3. Orient sensor's Y axis to North and measure α and $\emptyset$:

$$\alpha_Y = \underline{\hspace{2cm}} \text{ degrees}$$

$$\emptyset_Y = \underline{\hspace{2cm}} \text{ degrees}$$

4. Orient sensor's -Y axis to North and measure α and $\emptyset$:

$$\alpha_{-Y} = \underline{\hspace{2cm}} \text{ degrees}$$

$$\emptyset_{-Y} = \underline{\hspace{2cm}} \text{ degrees}$$